LUND UNIVERSITY

Exploring N-alicyclic quaternary ammonium functional polymers as hydroxide exchange membranes

Olsson, Joel

2020

Exploring *N*-alicyclic quaternary ammonium functional polymers as hydroxide exchange membranes

JOEL S. OLSSON | CENTRE FOR ANALYSIS AND SYNTHESIS | LUND UNIVERSITY

Exploring *N*-alicyclic quaternary ammonium functional polymers as hydroxide exchange membranes

Joel S. Olsson

LUND
UNIVERSITY

DOCTORAL DISSERTATION

by due permission of the Faculty Engineering, Lund University, Sweden.
To be defended at Kemicentrum, Lecture Hall K:C on May 8, at 13.15.

Faculty opponent
Dr. Ghislain David, L'Institut Charles Gerhardt Montpellier

Organization LUND UNIVERSITY	**Document name** Doctoral Dissertation
	Date of issue 2020-04-14
Author Joel S. Olsson	Sponsoring organization

Title and subtitle

Exploring *N*-alicyclic quaternary ammonium functional polymers as hydroxide exchange membranes

Abstract

As the global power generation is shifted toward renewable and intermittent sources, the importance of fuel cells and other energy storage and conversion devices is continually increasing. However, many of these technologies are still under development and further research is necessary before they can be implemented. This is the case for the hydroxide exchange membrane fuel cell (HEMFC), which has been identified as an important next-generation conversion technology. One under-developed and critical component of this technology, which is currently hampering its application, is the hydroxide exchange membrane (HEM). It consists of cationic polymers that conduct hydroxide ions and is essential to the performance and durability of the fuel cell. During prolonged fuel cell operation current HEMs tend to degrade due to an incompatibility between the cationic polymers and the hydroxide ions. To overcome this, continued exploration of new polymer architectures and chemistries is needed and that is where this thesis work comes in.

In this work, we have designed and synthesized different cationic polymers functionalized with *N*-alicyclic quaternary ammonium (QA) cations for use as HEMs. The overall focus of this thesis has been to explore the effect of different structural elements of the polymers, such as cation design and placement, on key properties of the HEMs. While extra emphasis was placed on the alkaline stability of the polymers, other *ex-situ* properties such as hydroxide conductivity, water uptake, morphology and thermal stability has also been studied. The scientific approach was constructed to highlight important structure-property relationships and gain other valuable insights that might aid the ongoing and future research on HEMs and HEMFCs.

The investigated polymers include poly(diallylammonium hydroxide)s prepared in radical initiated cyclopolymerizations, poly(arylene piperidinium)s prepared in superacid promoted Friedel-Crafts polycondensations and polystyrene functionalized in hydroxyalkylation reactions. HEMs with high hydroxide conductivity (>100 mS cm^{-1}) was obtained from all these polymers. A general finding observed while studying these materials was that the stability of *N*-alicyclic QA cations is very dependent on the conformational freedom of the ring. In contrast to studies on model compounds, when incorporated into a polymer the *N*-spirocyclic cation was consistently observed to be less stable than the monocyclic *N*,*N*-dimethylpiperidinium cation, and main pathway of degradation for both ions was *via* ring-opening β-hydrogen elimination.

Key words: hydroxide exchange membranes, anion, fuel cell, quaternary ammonium, structure-property relationship, alkaline stability, piperidinium

Classification system and/or index terms (if any)

Supplementary bibliographical information		**Language** English
ISSN and key title		ISBN 978-91-7422-738-3 (Print) ISBN 978-91-7422-739-0 (Digital)
Recipient's notes	**Number of pages** 215	Price
	Security classification	

Signature: 

Date 2020-03-24

Exploring *N*-alicyclic quaternary ammonium functional polymers as hydroxide exchange membranes

Joel S. Olsson

LUND
UNIVERSITY

Cover photo (front): illustration of an *N*-alicyclic quaternary ammonium functional polymer on a background by Kevin Phillips (from Pixabay).

Cover photo (back): blossoming magnolias in front of the Lund University main building, photography by Louise Larsson (from LU bildbank).

Funding information: The work present herein was funded by the Swedish Energy Agency (Energimyndigheten).

Faculty of Engineering, Department of Chemistry, CAS

ISBN 978-91-7422-738-3 (print)
ISBN 978-91-7422-739-0 (digital)

Printed in Sweden by Media-Tryck, Lund University, Lund 2020

Table of contents

Acknowledgments

The over 4.5-year journey to get to this point has been both challenging and rewarding. One thing is for sure though, without help, support and encouragement from the people around me, the work presented herein would not have been possible.

Patric, the supervisor who probably doesn't remember the last time he got a grant rejection letter, thank you very much for everything. Your door has always been open for discussions and guidance, and I almost always left your office motivated to try a new experiment or a new angle to solve arising problems.

A big thanks to **Huong**, our collaboration might have been a little unorthodox, but we both knew that we'd rather follow our own projects from start to finish, than getting involved too much. Thank you for your helpfulness and for not being afraid to tell me I'm being stupid.

To all past and present members of the polymer electrolyte membrane research subgroup, a big thank you!

To **Annika** and **Hai-Son**, who helped me get settled in the lab and office when I first started. To **Hannes**, for your, sometimes valued, monologues and strange way of always knowing if something in the lab needed my attention. To **Narae**, for valuable discussions on superacid polymerizations and for spicy noodles. To **Andrit**, for your positivity and always reminding me of "fika-time". To **Dong**, for understanding what I was trying to convey, even though I barely understood my own explanation. To **Pegah** and **Anuja,** who quickly learnt that I could not help as much as they had hoped, but still managed. And a good luck to our newest member **Oskar**.

There are many people who I have had the pleasure of getting to know during my time at Polymat and CAS, too many to mention them all. However, among them are a few that I connected extra well with and would like to express gratitude towards. Thank you, **Axel**, **Laura**, **Christoffer**, **Niklas**, **Kristoffer**, **Alexander**, **Daniel**, **Valtýr**, and **Robin** for making teaching, fika, lunch and everyday work-life more fun.

Friday lunches were always one of the high points of the week. Spending time with former n10 classmates (a.k.a. Dr. Nano), **Anders**, **Axel** x2 (x and y), **Calle**, **Emil**, **Erik**, **Malin**, **Marcus**, **Martin** and **Sara,** laughing about shared memories, discussing the future and exchanging PhD-life experiences was really wonderful.

A heartfelt thank you to my friends for their support and to my family who is always there whenever I need them. Even though my parents were not so sure about this

PhDing, the support was there, and I think they might even fully approve of it now. **Elin**, my fantastic wife, where would I be if I didn't have you to be silly with? I love you dearly and I look forward to the many years together we have in front of us.

Populärvetenskaplig sammanfattning

En polymer är en stor kemisk molekyl uppbyggd av sammankopplade mindre enheter, monomerer, och utgör grunden för de material som till vardags kallas för plast eller gummi. Genom att ändra en polymers kemiska uppbyggnad kan dess materialegenskaper skräddarsys och användas för väldigt olika ändamål. Exempelvis så är både tuggummi och bowlingklot baserade på polymerer. Den typ av polymerer som behandlats i denna avhandling är så kallade jonomerer och består av polymerkedjor med laddade grupper (joner) på.

Ett stort användningsområde för jonomerer är som membran i polymerbränsleceller, vilka ses som en viktig del i ett framtida fossilfritt samhälle. I dessa omvandlas energi i ett bränsle, i form av kemiska bindningar, till elektricitet genom en elektrokemisk process. I den vanligaste processen omvandlas vätgas och syrgas till vatten och elektrisk energi. Förutom värme, är den enda biprodukten eller avgasen alltså vatten. För att processen ska fortgå måste både joner och elektroner transporteras mellan bränslecellens olika sidor (elektroder; plus- och minuspol). Elektronerna som bildats leds ut från cellen för att driva exempelvis en elmotor, medan jonerna transporteras genom jonomermembranet. Vilken jon som transporteras beror på designen av bränslecellen. Vanligast är protoner (H^+) eller hydroxidjoner (OH^-).

I en konkurrenskraftig bränslecell måste den elektrokemiska processen vara effektiv och kunna fortgå under lång tid. För att uppnå detta krävs att alla komponenter och delar av bränslecellen är optimerade, hållbara och ger så låga förluster som möjligt. I den bästa av världar ska bränslecellen köras under många tusen timmar, gärna vid en hög temperatur (80 – 100 °C), då detta påskyndar de elektrokemiska processerna. En av de mer kritiska komponenterna för att uppnå detta är jonomermembranet och det är just forskning kring och utveckling av denna komponent som varit fokus i detta arbete. De jonomermembran vi undersökt är av den typ som transporterar hydroxidjoner, även kallat anjonbytarmembran, och dessa används i en typ av alkaliska bränsleceller, som körs vid högt pH. En stor fördel med alkaliska bränsleceller, jämfört med bränsleceller som körs under sura betingelser, lågt pH, är att man potentiellt kan använda mindre ädla (billigare och vanligare) metaller som katalysator. Teknologin kan därav bli både billigare och mer tillgänglig.

Alkaliska bränsleceller är fortfarande i utvecklingsstadiet och flera komponenter behöver förbättras innan kommersialisering, däribland jonomermembranet. Två egenskaper med utvecklingspotential är jontransporten genom membranet och jonomerens livslängd och hållbarhet vid höga temperaturer i alkalisk miljö. Det är

specifikt det sistnämnda som varit fokus i detta arbete, där vi på molekylär nivå designat jonomerer för att sedan syntetisera och studera egenskaperna hos dessa material.

Jonomererna som presenteras i detta arbete bär alla joner av cyklisk karaktär, då det påvisats i tidigare studier att denna typ av jon har en väldigt hög stabilitet i alkalisk miljö. Svårigheten med cykliska joner är att de är besvärliga att inkorporera på polymerkedjor och det kan krävas många och dyra synteser för att uppnå detta. Genom smart molekyldesign och syntes har vi dock tagit fram tre olika typer av jonomerer bärande cykliska joner, och av dessa tillverkat och studerat jonomermembran. Flera av membranen visade sig ha väldigt hög alkalisk stabilitet och resultaten ligger till gagn för framtida bränslecellsforskning.

List of appended papers

This thesis is based on the following papers:

I. **Poly(*N*,*N*-diallylazacycloalkane)s for Anion-Exchange Membranes Functionalized with *N*-Spirocyclic Quaternary Ammonium Cations**
Joel S. Olsson, Thanh Huong Pham, and Patric Jannasch
Macromolecules **2017,** *50*, 2784-2793

II. **Poly(arylene piperidinium) Hydroxide Ion Exchange Membranes: Synthesis, Alkaline Stability, and Conductivity**
Joel S. Olsson, Thanh Huong Pham, and Patric Jannasch
Adv. Funct. Mater. **2018**, *28*, 1702758

III. **Poly(arylene alkylene)s with pendant *N*-spirocyclic quaternary ammonium cations for anion exchange membranes**
Thanh Huong Pham, **Joel S. Olsson**, and Patric Jannasch
J. Mater. Chem. A, **2018**, *6*, 16537

IV. **Tuning poly(arylene piperidinium) anion-exchange membranes by copolymerization, partial quaternization and crosslinking**
Joel S. Olsson, Thanh Huong Pham, and Patric Jannasch
J. Membr. Sci. ***2019****, 578,* 183-195

V. **Functionalizing polystyrene with *N*-alicyclic piperidine-based cations *via* Friedel-Crafts alkylation for anion-exchange membranes with improved alkaline stability**
Joel S. Olsson, Thanh Huong Pham, and Patric Jannasch
Submitted (Jan 2020) - *Macromolecules*

My contributions

I I planned and performed all the experimental work. I wrote the first draft of the paper.

II I planned and performed a vast majority of the experimental work. I wrote the first draft of the paper.

III I took an active part in planning experimental work and discussing ideas. I did not perform any lab work. I participated actively in the later stages of the project, with *e.g.* data analysis and proofing.

IV I planned and performed all the experimental work. I wrote the first draft of the paper.

V I planned and performed all the experimental work. I wrote the first draft of the paper.

Publications not included

VI *N*-Spirocyclic Quaternary Ammonium Ionenes for Anion-Exchange Membranes
Thanh Huong Pham, **Joel S. Olsson**, and Patric Jannasch
J. Am. Chem. Soc. **2017**, *139*, 2888-2891

VII Effects of *N*-alicyclic cation and backbone structure on the performance of poly(terphenyl)-based hydroxide exchange membranes
Thanh Huong Pham, **Joel S. Olsson**, and Patric Jannasch
J. Mater. Chem. A **2019**, *7* (26), 15895-15906

VIII Ether-free polyfluorenes tethered with quinuclidinium cations as hydroxide exchange membranes
Andrit Allushi, Thanh Huong Pham, **Joel S. Olsson**, and Patric Jannasch
J. Mater. Chem. A **2019**, *7* (47), 27164-27174

IX Fuel cell evaluation of anion exchange membranes based on poly(phenylene oxide) with different cationic group placement
Annika Carlson, Björn Eriksson, **Joel S. Olsson**, Göran Lindbergh, Carina Lagergren, Patric Jannasch, Rakel Wreland Lindström
Sustain. Energy Fuels – Accepted: doi.org/10.1039/C9SE01143A

Abbreviations

AEM	anion-exchange membrane
AEMFC	anion-exchange membrane fuel cell
AFC	alkaline fuel cell
APS	ammonium persulfate
ASU	6-azonia-spiro[5.5]undecane, *N*-spirocyclic cation
DADMAC	diallyldimethylammonium chloride
DCM	dichloromethane
DIPEA	*N*,*N*-diisopropylethylamine
DMP	*N*,*N*-dimethylpiperidinium, monocyclic cation
DMSO	dimethylsulfoxide
E1	unimolecular elimination
E2	bimolecular elimination
FC	fuel cell
HEM	hydroxide exchange membrane
HEMFC	hydroxide exchange membrane fuel cell
IEC	ion-exchange capacity (meq. g^{-1} or mmol g^{-1})
IEM	ion-exchange membrane
MEA	membrane electrode assembly
MOFC	molten carbonate fuel cell
mPip	*N*-methyl-4-piperidone
NMP	*N*-methyl-2-pyrrolidone
PAA	poly(arylene alkylene)
PAPipQ	poly(arylene piperidinium)
PBI-O	polybenzimidazole
PEMFC	proton-exchange membrane fuel cell
Pip*t*OH	2-(piperidine-4-yl)propane-2-ol
PSU	polysulfone
QA	quaternary ammonium
S_N2	bimolecular nucleophilic substitution
SOFC	solid-oxide fuel cell
TFA	trifluoroacetic acid
TFSA	triflic acid/trifluoromethanesulfonic acid

Symbols

d	characteristic separation distance
λ	water content, $[H_2O]/[OH^-]$ or $[H_2O]/[QA]$
$[\eta]$	intrinsic viscosity
σ	ion conductivity
q	scattering vector

1 Context and scope

The current worldwide electric generation capacity is estimated to be about 25 x 10^6 GWh,[1] and the energy demand is still growing. Unfortunately, it is accompanied by an increase of greenhouse gases in the atmosphere[2], making it impossible to meet the growing energy demand with combustion of more fossil fuels. To limit the global warming to below 2 °C (Paris Agreement), the global energy demand year 2050 must not be greater than that of 2015 and two-thirds of the energy from primary sources must come from renewables.[3] To achieve this, focus has shifted to the development of alternative energy technologies that would offer sustainable energy to all economic sectors globally.[4] Among these technologies are energy storage and conversion devices[5], which store electrical energy either electrochemically (*e.g.* batteries)[6] or by conversion to chemical bonds (*e.g.* water electrolysis).[6, 7] Implementation of these technologies would make it possible to decouple the electricity generation from its demand by releasing or converting the stored energy to electricity (*e.g.* using fuel cells) when required. Without this kind of infrastructure, intermittent and less reliable primary energy sources, like wind and solar energy, cannot be efficiently utilized on a large scale to power the world.[8] In order to establish such a comprehensive energy infrastructure, the conversion and storage devices, and their components, need to be further developed.

A conversion device with great potential is the fuel cell. It electrochemically converts energy stored in chemical bonds to electricity and offers high conversion efficiencies as well as zero emissions with great scalability and cogeneration possibilities.[9, 10] Today, several different types of fuel cells exists, such as phosphoric acid fuel cells, solid oxide fuel cells, alkaline fuel cells as well as polymer electrolyte membrane fuel cells.[10] The latter has received a lot of attention as a promising power source for the next generation of vehicles. The topic of this thesis work is related to the development of a crucial component of this kind of fuel cell, namely its polymeric electrolyte membrane, which is a type of ion-exchange membrane. The properties of this membrane strongly affect both the output and lifetime of the fuel cell itself. Due to the harsh environment of fuel cell operation, the requirements of high ionic conductivity and structural integrity over thousands of hours are difficult to achieve.

Presented in this thesis is the development, preparation and characterization of polymers tailored to withstand the alkaline environment and elevated temperatures of hydroxide exchange membrane (HEM) fuel cell operation. On basis of the results in a recent publication, where *N*-alicyclic quaternary ammonium cations were found

to be exceptionally stable[11], synthetic procedures to prepare polymers carrying this type of cationic moieties were developed and the subsequently cast HEMs were characterized with special focus on chemical stability.

No fuel cell tests of the prepared materials are included in this work

2 Introduction

Ion exchange membranes (IEMs) typically consist of a hydrophobic polymer functionalized with immobilized ionic groups and their mobile counter-ions.[12] The inherent osmotic pressure of the IEM causes absorption of water into the membrane, which allows the ions to dissociate and enables controlled diffusion of the counter-ions through the membrane.[12] Depending on the charge of the transported ion, an IEM is classified as either an anion-exchange membrane (AEM) or a cation ditto.[12] IEMs have found use in several applications related to energy conversion and storage, *e.g.* in redox flow batteries[13], reverse electrodialysis[14], water electrolysis[15] and polymer electrolyte membrane fuel cells[16], all in which the IEM functions as a polymer electrolyte membrane. In this work, research has been focused solely on alkaline AEMs or hydroxide exchange membranes (HEMs) for fuel cells. Thus, the introduction will be focused on the description of fuel cells, membrane requirements and recent advances in the field of HEMs.

2.1 Fuel cells

A fuel cell is an electrochemical device that continuously converts the chemical free energy of a gas or a liquid into electrical energy *via* redox reactions.[17] In the most simple case, H_2 (fuel) is oxidized, while O_2 (oxidant) is reduced to form H_2O, electricity and heat. The produced electrical energy can be used to power *e.g.* an electric car motor. Vehicles powered this way can both be refueled as quickly as current petrol cars and be zero-emission, depending on how the fuel is produced.

Similar to a battery cell, the fuel cell consists of two electrodes (anode, cathode) separated by an electrolyte.[17] Through the years, a variety of fuel cells have been developed and they are normally classified according to the type of electrolyte used. For example, solid oxide fuel cells (SOFCs) and molten carbonate fuel cells (MCFCs) have electrolytes consisting of solid oxides and molten carbonates, respectively. They are both examples of high temperature fuel cells and operate at temperatures up to 1000 °C, which makes them appropriate for stationary applications.[17] Both alkaline fuel cells (AFCs) and polymer electrolyte membrane fuel cells are examples of low temperature fuel cells.[17] The AFC has aqueous KOH as electrolyte while an IEM functions as the electrolyte in the latter.[17] In comparison with other fuel cell technologies, the polymer electrolyte membrane fuel cell is more suitable for transportation applications due to its high energy density and the low operating

temperature.[17] The polymer electrolyte membrane fuel cells are divided into to two distinctly separate categories depending on which the transported ion is, protons or hydroxide ions.

2.1.1 Proton-exchange membrane fuel cells (PEMFC)s

PEMFCs were first developed in the US during the space age in the 1960's and have since then seen significant advances.[10] Today, PEMFCs can be found in several commercially available vehicles (Toyota Mirai, Hyundai Tucson, etc.), but also in stationary applications.[18] A general overview of how a single PEMFC functions is shown in **Figure 1a** and the electrochemical reactions that occur are the following:

$$\textbf{Anode (oxidation):} \quad \mathbf{H_2 \rightarrow 2\,H^+ + 2e^-} \qquad E^0 = 0\ \text{V}$$

$$\textbf{Cathode (reduction):} \quad \mathbf{½\,O_2 + 2\,H^+ + 2e^- \rightarrow H_2O} \qquad E^0 = 1.23\ \text{V}$$

$$\textbf{Total:} \quad \mathbf{½\,O_2 + H_2 \rightarrow H_2O} \qquad E^0 = 1.23\ \text{V}$$

The operating temperature of a PEMFC is typically limited to between 50 and 100 °C, due to limitations of the proton-exchange membrane (PEM).[17] At these comparatively low temperatures, reaction rates are rather sluggish and in order for a PEMFC to function adequately, costly and rare platinum catalysts are employed to speed up the electrochemical processes.[10] Even though much effort and some

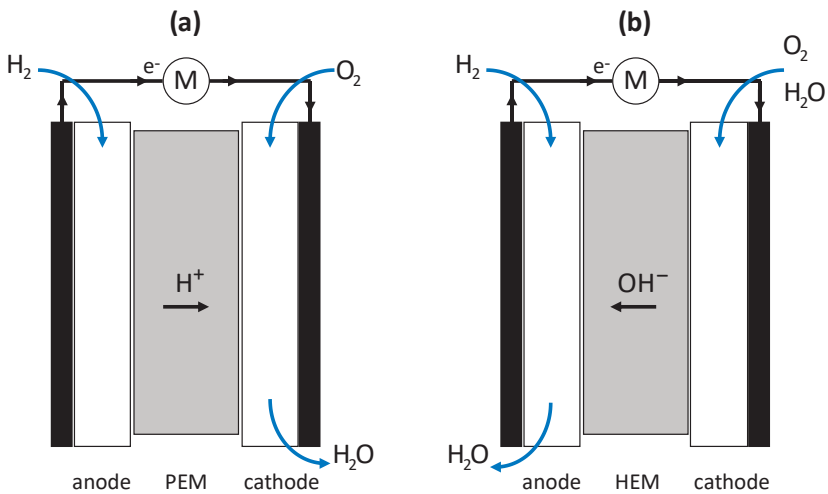

Figure 1. Schematic of two different single fuel cells powering a motor (M), one with an acidic electrolyte (PEM) (a) and the other with an alkaline one (HEM) (b). In both cases anode and cathode consist of a gas diffusion layer, a catalyst layer and a bipolar plate.

progress has been made to replace and decrease the platinum loading[19, 20] and to recycle the platinum[21], further development is needed in order for PEMFCs to be a serious alternative to combustion engines in automotive applications.

One of the most commonly used PEMs today was developed already in the 1960s by DuPont.[22] It is a copolymer consisting of a Teflon-based backbone with perfluorinated sidechains terminated with sulfonic acid groups, as shown in **Figure 2**, and was originally developed as a separator membrane transporting Na^+ in the chlor-alkali process.[23] This polymer goes by the trade name Nafion and is still seen as a benchmark in the field.[23] It combines a very hydrophobic fluorinated backbone carrying fluorinated side chains capped with superacidic perfluorosulfonic acid groups. A combination that promotes phase separation and offers a high proton conductivity at low hydration levels.[24] The main drawbacks of Nafion, in addition to its high price, are dehydration as well as its poor mechanical and chemical stability at high temperatures.[25] In 2013 Nafion was reported to be, by far, the most expensive single component of a fuel cell stack.[25] However, even after decades of research on alternate PEMs, Nafion continues to be the most used PEM in energy conversion and storage devices.[26]

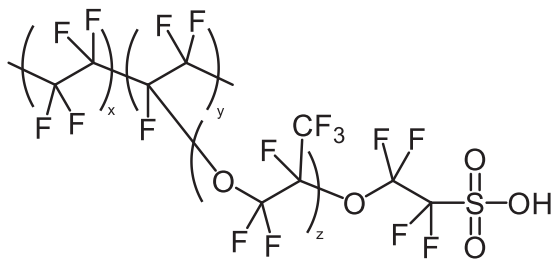

Figure 2. Molecular structure of Nafion®.

2.1.2 Alkaline and hydroxide exchange fuel cells

Alkaline fuel cells (AFCs) that use aq. KOH as electrolyte were also developed during the space age.[17] Compared to the acidic PEMFC, AFCs have a significant advantage because operation in a high pH environment offers advantageous reaction kinetics.[17] This makes it possible to replace the Pt-group catalysts required in *e.g.* PEMFCs with less rare and cheaper alternatives, such as Fe or Ag, in alkaline systems.[17, 27] However, there are two major drawbacks for this type of fuel cell. First, leakage of highly corrosive and hot KOH solution could possibly damage machinery and injure humans. Second, electrolyte poisoning by CO_2 decreases the efficiency of the fuel cell by physically obstructing the mass transport.[17] In contact with OH^- ions

in the cell, CO_2 from ambient air reacts to form HCO_3^- and CO_3^{2-}, which precipitates together with K^+ causing pore blockages in the gas diffusion layer.[17]

Quite recently, another type of fuel cell operating under alkaline conditions, namely, the hydroxide exchange membrane fuel cell (HEMFC), also called the anion-exchange membrane fuel cell (AEMFC), started to receive a lot of attention.[28] This interest arose because the HEMFC has the potential to combine the advantages of both the PEMFC and the AFC.[27, 29] That is, the leakage-free solid electrolyte of the PEMFC and the faster reaction kinetics in alkaline media of the AFC, potentially making it both safe and cheap(er).[30] On top of this, since the cationic moieties in these membranes are covalently attached to the polymer, they cannot co-precipitate with formed carbonates and cause pore blockages, as observed in AFCs.[17]

An assembled HEMFC is very similar to a PEMFC, and also functions in a similar way as illustrated in **Figure 1b**. Nevertheless, there are several important differences between them, such as the direction of ion transport, water management and the presence of the OH^- ion, which is both a base and a nucleophile.[29] The electrochemical reactions in alkaline media are:

Anode (oxidation):	$\mathbf{2\,OH^- + H_2 \rightarrow 2\,H_2O + 2\,e^-}$	$E^0 = -0.83$ V
Cathode (reduction):	$\mathbf{½\,O_2 + H_2O + 2\,e^- \rightarrow 2\,OH^-}$	$E^0 = 0.40$ V
Total:	$\mathbf{½\,O_2 + H_2 \rightarrow H_2O}$	$E^0 = 1.23$ V.

The research on HEMFCs is still quite young and the foundation of the field was laid in 2006 by Varcoe with a publication on the first all-solid-state HEMFC without additional base dopant.[31] A couple of years later, Zhuang et al. presented the first Pt-free HEMFC[32] and from there, the field expanded rapidly and has since advanced tremendously. The advances can be followed by studying some of the many comprehensive reviews written on the topic.[27-30, 33-38] For example, the targeted *ex-situ* OH^- conductivity of the HEM has increased from 10 mS cm^{-1} before 2010[28] to 100 mS cm^{-1},[35] including several reports on HEMs that approached or reached a conductivity of 200 mS cm^{-1}.[39-41] In connection with this, the highest reported peak power for a H_2/O_2 hydroxide membrane electrode assembly (MEA) was, at the time of writing, 3.4 W cm^{-2} with a Pt-loading of 1.5 mg cm^{-2} reported in 2019 by Kohl et al.[42] This is more than a 60-fold increase in power output compared to the early MEAs prepared by Varcoe in 2006.[31]

Even though the potential of the HEMFCs is huge, there are some drawbacks and issues that need to be addressed before realization of a commercial product. To surpass current PEMFCs equipped with Nafion, an HEMFC should be cheaper, but

still have a similar performance. A crucial component to achieve this is the HEM, which to a large extent determines the lifetime and performance of the whole fuel cell.[29]

2.2 Hydroxide exchange membranes

An HEM is a solid electrolyte membrane that consists of polymers functionalized with cationic groups (typically quaternary ammonium (QA)) and OH^- as the mobile counter ion.[43] Its main purpose is to transport OH^- ions between the fuel cell electrodes, while isolating both the current and the reactant gases at respective electrode. The fundamental requirements of HEMs for fuel cells include: high hydroxide conductivity, mechanical integrity and good separation properties, as well as thermal and chemical stability against radicals, bases and nucleophiles.[29, 43] The ionic conductivity of the membrane determines the number of electrons produced in the fuel cell (1 electron per monovalent ion). Thus, an insufficient OH^- conductivity will limit the fuel cell power density. The water content of the HEM is vital for the ion transport, but a too large water uptake might instead lead to a dilution effect, which reduces the OH^- conductivity.[44] Excessive amounts of water might also cause the mechanical properties of the HEM to suffer, which can impair the separation properties and enable gas crossover or short circuiting.[29] The last two points, thermal and chemical stability, are related to the lifetime of the membrane in the harsh conditions of fuel cell operation. Even slow degradation or decomposition will over time decrease the efficiency of the fuel cell. In a best case scenario, membrane degradation only leads to a small voltage loss, but in some cases it might also cause the fuel cell to break down.

The advantages of switching from acidic PEMs to alkaline HEMs have been discussed previously. However, changing the transported ion from H^+ to OH^- also introduces new obstacles to overcome.[43] One related to ionic conductivity and one to membrane durability. First, the diffusion coefficient and mobility of the OH^- ion are intrinsically lower than of H^+ in water, due to the different size and solvation behavior of the anion.[44] In addition, QA groups are less dissociated than typical corresponding sulfonic acid groups in PEMs ($pK_b \sim 4$ compared to $pK_a < -1$) at low hydration levels.[43] Together these two attributes make the OH^- conductivity for HEMs lower than corresponding H^+ conductivity for PEMs. The second issue is related to the chemical stability of the HEM in aqueous alkaline media, also called the alkaline stability.[11, 45-47] In contrast to the rather unreactive H^+, the OH^- ion functions both as a nucleophile and base. Within the membrane this reactive specie is surrounded by large organic molecules carrying plenty of decent leaving groups. Hence, at the

elevated temperature of HEMFC operation, where the reactivity of the OH^- ion is increased, chemical stability issues arise.[29, 30] Depending on temperature and humidity (degree of solvation of the OH^- ion), degradation rates and mechanisms can vary, even for the same polymer sample.[48] This further emphasizes research on polymers, HEMs and their stability in alkaline media in order to gain valuable structure-property relationships and to better understand the degradation phenomena.

A more in-depth explanation of HEMs, their properties, design and synthesis will now follow.

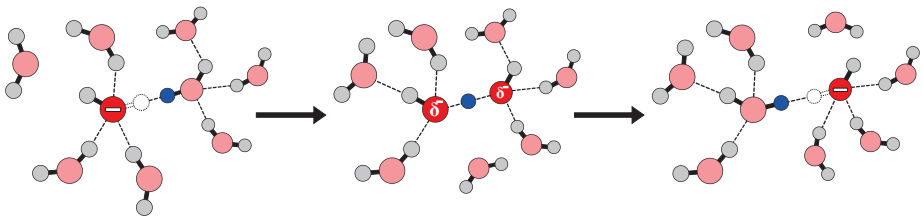

Figure 3. Structural diffusion (Grotthuss mechanism) of OH^- in liquid water with the transported hydrogen (blue) and proton hole (white) included. Adapted from Tuckerman et al.[49]

2.2.1 Ion transport, conductivity, water uptake and morphology

Transport of OH^- ions in water occurs *via* the same mechanism as H_3O^+, but differ from other ions.[50] In liquid water, the presence of H_3O^+ and OH^- can be pictured as opposite defects in a hydrogen bond network (protons and proton holes, respectively).[50] As the dynamic O-H bonds form and break, the defects move between adjacent molecules and are in that way transported through the network as shown in **Figure 3**. This type of diffusion is called structural diffusion and occurs *via* the Grotthuss mechanism.[51] It is the main transport mechanism for both H_3O^+ and OH^- in water and is the underlying reason for the anomalously high mobility of H_3O^+ and OH^- in water compared to other ions.[50] Customary diffusion, also called vehicular or hydrodynamic diffusion, which is the normal mode of transport for most ions, also contributes to the diffusion of both H_3O^+ and OH^-.[52] Despite the mechanistic similarity, the total diffusion of H_3O^+ is approximately twice that of OH^- in liquid water.[44] As mentioned earlier, this is related to the size and different solvation behavior of the ions.[44, 53] For example, structural diffusion is retarded because OH^- can be stabilized by a hyper-coordinated solvation structure, which "discourages" proton transfer, according to Wu et al.[53]

The above also applies for ion transport in HEMs and PEMs, which is governed by two factors: the ion-exchange capacity (IEC) of the membrane and the mobility of the ions.[54] A sufficiently hydrated HEM can exhibit an ion conductivity within a

factor 2 of a PEM with the same number of charge carriers per gram polymer (IEC).[44] However, at lower hydration levels the OH^- conductivity decreases drastically due to a reduced degree of ion dissociation.[44] Thus, to achieve similar performance to a PEM, HEMs must have well hydrated ions (high mobility) and a higher IEC. To accommodate the high IEC, the HEM must withstand the increased osmotic pressure and avoid excessive water uptake, *e.g.* by employing polymers of high molar mass and/or implementing a phase separated morphology.[29, 55]

In addition to the presence of water and dissociated ions within the HEM (placed in an external electrical field), percolation is also needed for the ions to be transported through the membrane.[29] That is, the connectivity of aqueous phase must be developed enough to allow the ions to travel across the full width of the membrane. However, percolation should not come at the expense of the mechanical integrity of the HEM. At high water uptake (>100%; mass of water > mass of dry membrane), percolation and ion transport are seldom a problem, but depending on polymer structure and molar mass, the mechanical properties might be compromised. Thus, it is beneficial to achieve percolation already at low water uptake.

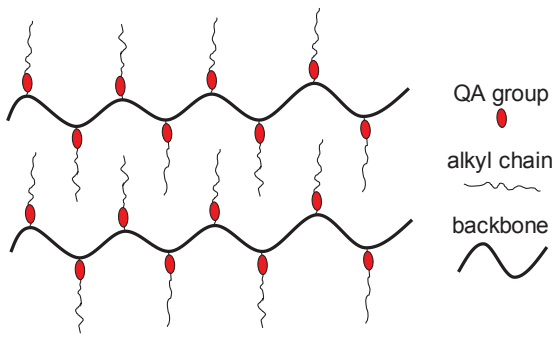

Figure 4. A phase separated lamellar structure of a comb-shaped polymer used as an HEM. Adapted from Binder et al.[56]

A connection between the presence of phase segregated ion rich domains (ionic clusters) in a dry membrane, which aids percolation when hydrated, and high ionic conductivity at limited water uptake has been demonstrated.[39, 54, 56-58] By clever polymer design, *e.g.* using alkyl extenders[56, 57] or spacers[57, 58], the formation of these ionic clusters can be facilitated. As the membrane takes up water, the ionic domains will swell and form an interconnected hydrated phase enabling high OH^- conductivity, even at low water uptake (<50%). Shown in **Figure 4** is an example of a polymer designed to phase separate. The alkyl chains of this comb-shaped polymer, reported by Binder et al., caused segregation and formation of an ordered lamellar structure.[56] Compared to a polymer with no clear clustering, HEMs based on this type

of polymer architecture showed much higher conductivity at lower water uptake.[56] Another way to facilitate phase separation is to prepare polymers where the QA groups are concentrated to certain segments within the polymer structure (*i.e.* multicationic repeating units or block copolymers).[29, 59] However, placement of ions in too close proximity might lead to an incomplete ion dissociation and therefore a decrease in ion conductivity.[44, 60] The phase separation and morphology of dry HEMs is typically studied using small angle X-ray scattering techniques.

In recent years, HEMs found in literature often exhibit OH^- conductivity that surpass 100 mS cm^{-1} and have started to rival those measured for PEMs.[30] However, achieving high conductivity at limited/low water uptake (<50%) is still challenging and requires both a high IEC, rational polymer design and polymers of high molar mass. Since the work presented in thesis has been more focused on the exploration and development of alkali-stable HEMs and studying structure-property relationships with this focus, achieving high conductivity at low water uptake would only be a bonus.

2.2.2 The polymer backbone

There are a vast number of different polymers that can be used to form membranes, but only a limited number that have the potential to fulfill the earlier stated requirements of an HEM. Fundamentally, the polymer backbone must provide the HEM with good mechanical stability at the operating temperature by withstanding the osmotic pressure and limiting the difference in dimensional swelling between dry and wet state.[29] Thereby keeping the mechanical stress on the membrane during fuel cell operation to a minimum. On top of this, the backbone should also possess a high thermal and chemical stability. To accommodate all the requirements stated above, a typical backbone has a high glass transition temperature (T_g) and is highly aromatic.

In the early stages of HEM research, previously gathered knowledge from studying PEMs was directly implemented into the new field of membrane research for HEMFCs. Thus, many early HEMs were based on polysulfone (PSU) backbones that were designed and functionalized various ways.[61, 62] An example of a PSU is displayed in **Figure 5a**. In addition to the earlier mentioned attributes, these polymers also provide good film forming properties and can easily be modified chemically, either pre- or post-polymerization. However, HEMs based on PSUs often performed very poorly in alkaline solutions, wherein they tend to degrade rapidly. Both the aryl ether bonds and the quaternary carbons present in the PSUs can be activated for hydrolysis.[63-65] Moreover, attaching a cationic group in the benzylic position further destabilizes the backbone and causes polymer degradation *via* chain cleavage, as shown in **Figure 5c**.[63-67]

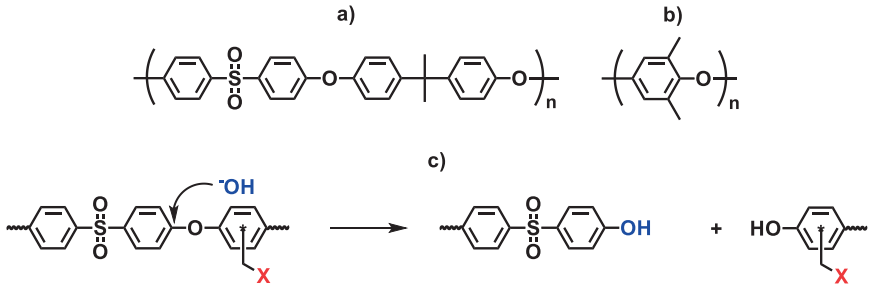

Figure 5. Examples of polymer backbones containing aryl ether bonds, a) PSU and b) PPO. c) Chain scission in alkaline media of an activated ether bond in a functionalized PSU.[63, 68] X corresponds to an electron withdrawing group, *e.g.* a QA group.

Since then a variety of other polymer backbones have been explored. Among them is poly(*p*-phenylene oxide) (PPO) (**Figure 5b**), which is a commercially available polymer that offers possibilities similar to the PSUs, while providing a better alkaline stability.[67] Our group have in recent years worked a lot with PPO, especially with preparation of HEMs from bromoalkylated PPO made using lithiation chemistry.[69-71] Some of the experience of working with PPO was utilized in Paper I to prepare crosslinked HEMs from pre-functionalized PPO and *N*,*N*-diallylpiperidinium chloride.

In a recent study by Bae et al., functionalized PPO was also found to degrade *via* chain scission of the backbone in alkaline solution at elevated temperature.[68] Even though the study showed that unsubstituted PPO possessed a high alkaline stability, it was also shown that the molar mass of functionalized PPO decreased after exposure. This effect was observed for PPO functionalized with heteroatoms attached in benzylic position as well as *via* alkyl chain. The degradation mechanism could not be conclusively elucidated, but was assumed to be similar to cleavage of the ether bonds observed for PSUs (**Figure 5c**).[63]

Even though PPO is still a popular backbone for HEM research, focus has shifted to the implementation of more suitable ether-free aromatic polymer backbones. Because of their lack of vulnerable ether groups, these backbones are not cleaved as easily and possess a higher stability towards the OH^- ion. Four different examples of such backbones prepared in four types of polymerizations are shown in **Figure 6**. They include, a) poly(quinquephenylene-fluorene)s prepared in Ni-mediated Yamamoto coupling polymerizations[72], b) poly(phenylene-fluorene)s prepared in Pd-catalyzed Suzuki coupling polymerizations[73], c) poly(arylene alkylene)s (PAA) prepared in superacid mediated polyhydroxyalkylations[74-82] and d) poly(phenylene)s prepared in Diels-Alder polymerizations[83, 84].

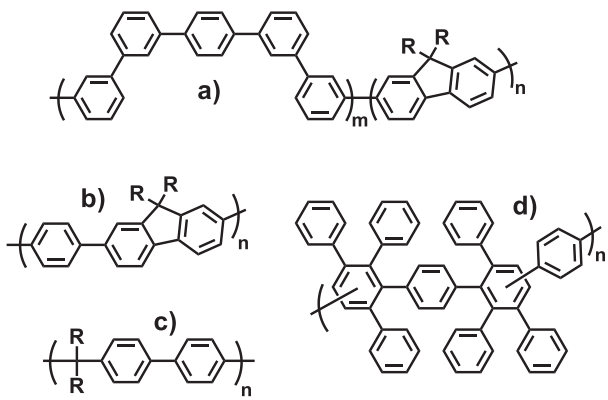

Figure 6. Examples of suitable ether-free aromatic polymer backbones used for HEMs found in literature: a) poly(quinquephenylene-fluorene)[72], b) poly(phenylene-fluorene)[73], c) poly(arylene alkylene) (PAA)[74-82] and d) polyphenylene[83, 84].

The examples above include only highly aromatic polymer backbones with high T_g. However, many other less rigid ether-free backbones have also been used for HEMs, for example, styrene-ethylene-butylene-styrene block copolymer (SEBS)[85-90], poly(norbornene)[42, 91-93], polystyrene (PS)[94] and polyethylene[95-100]. Because of their much less rigid backbone, HEMs based on these polymers tend to be softer and exhibit a larger water swelling at a given IEC compared to those based on more rigid backbones. To avoid an excessive dimensional swelling and to improve the mechanical integrity of HEMs based on these backbones, crosslinking and blending are commonly used strategies.[42, 85, 87, 93, 94]

HEMs based on PPO, PAA and PS backbones are included in this thesis work.

2.2.3 The cation

With a suitable polymer backbone identified, another, and perhaps, more difficult task is to determine what type of cation to use. A suitable cation should be alkali-stable, hydrophilic and possess a good oxidative and voltage stability.[29, 101] Hence, the cation should be stable towards hydroxide ions at elevated temperature without compromising its hydrophilic character. Since many strategies to increase the structural integrity of the cation is based on steric protection, its hydrophilicity is often sacrificed for an improved alkaline stability.[102-105] This may likely decrease both the water uptake and ion conductivity of the HEM, leading to a lower power output of the FC.[106] Thus, care has to be taken when designing and selecting cation. On top of this, the cation must be both stable towards reactive oxidants and not involved in their formation.[29, 35] Some cations have been shown to catalyze the formation of reactive oxygen species (*e.g.* superoxide radicals).[107] The typical

Fenton's reagent, used in the assessment of the oxidative stability for PEMs, cannot be used for HEMs, since the relevant radical species are not formed in alkaline media.[35] Instead, *in-situ* durability performance tests are preferred.[29]

In the search for high-performance HEMs a wide variety of cations has been synthesized and investigated, such as QA cations, sterically protected phosphonium moieties and transition metal complexes with large ligands (**Figure 7**).[11, 46, 80, 99, 103-105, 108-112] The bottom two examples in **Figure 7** are examples of larger and more complex ions. Metallocene cations typically require quite expensive synthesis, counteracting the main advantage of platinum-free HEMFCs, which is the potential low cost. Even though certain phosphonium ions have shown interesting properties[112], the high molecular weight of these bulky cations can make them difficult to implement.[29] Instead, QA cations are typically preferred and have been studied extensively. They are often commercially available or easily synthesized, as well as low molecular weight and facile to attach onto polymer backbones.[113] The most commonly encountered cation in literature is based on trimethylamine (TMA), i.e. benzyl-TMA or alkyl-TMA[57, 58, 85, 86, 114]. It is with basis in these facts the QA type cation was selected as the cation of choice in this work.

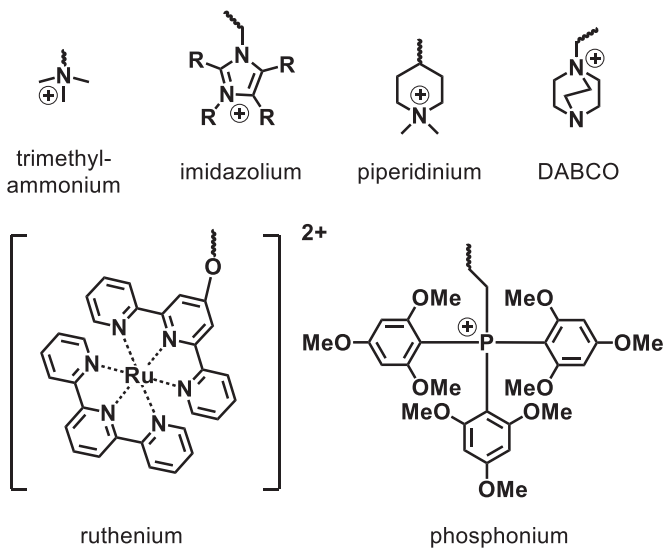

Figure 7. A few types of cationic moieties from recent research. The top row consists of different QA groups (TMA[57, 58, 75, 95], imidazolium[46, 99, 103-105], piperidinium[11, 76, 80, 94, 96, 108, 109], DABCO[110]), in the bottom one more exotic ones are displayed (ruthenium[111] and phosphonium[112]). The counter-ions have been left out for clarity.

QA Cation stability and degradation

The main degradation pathways of QA groups in the presence of OH^- ions are *via* nucleophilic substitution or β-elimination reactions (**Figure 8a**).[27, 33, 113] Bimolecular nucleophilic substitution (S_N2) occurs *via* a nucleophilic attack on an α-carbon resulting in a loss of charge and formation of an alcohol and a tertiary amine.[115, 116] The reaction proceeds *via* a trigonal bipyramidal transition state and results in an inversion of the stereochemistry. [115-117] β-elimination of a QA cation (referred to as Hofmann elimination) is the abstraction of a proton in the β-position to the charged center producing an alkene, a tertiary amine and water.[115] This reaction can only occur if the leaving group is positioned in an anti-periplanar (*trans*) conformation in regards to the abstracted proton and the formed alkene is the least substituted/stable one (Hofmann's rule).[115] The broken σ bonds are then correctly aligned to form a π bond, as can be seen in transition state in **Figure 8b**. However, sterically hindered QA cations having only *cis*-*β*-hydrogens (*trans* conformation hindered) may instead degrade *via* a two-step *β*-carbanion mechanism (E1cb).[118]

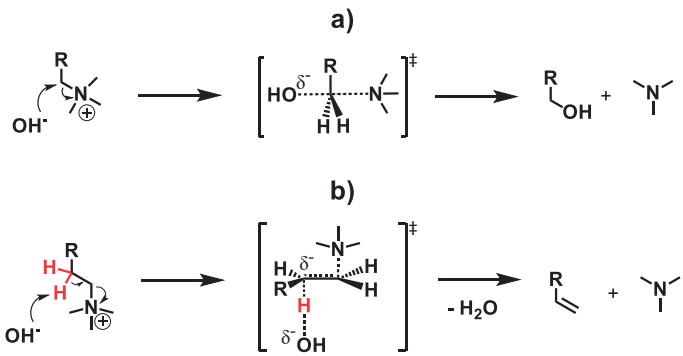

Figure 8. Illustration of nucleophilic substitution (S_N2) (a) and Hofmann elimination (b) of a QA group, including transition states. These two are the most prominent degradation pathways for commonly used QA groups.

Even though the above mentioned mechanisms constitute the most commonly encountered degradation pathways of QA compounds, other routes exist. Pyridine type cations degrade almost instantly *via* ortho attacks.[119] For benzylic QA groups (*e.g.* benzyl-TMA) degradation *via* ylid formation (*e.g.* Sommelet-Hauser and Stevens rearrangements) have been observed.[120-122] Imidazoliums, resonance stabilized ammonium type cations, tend to degrade *via* a nucleophilic addition-elimination pathway if no bulky substituents have been attached.[123] For all examples of degradation above, it is expected that the total Gibbs free energy of the starting materials (QA and OH^-) is higher ($\Delta G < 0$) than that of the degradation products

(alcohol, alkene, alkane, water, etc.) and stabilization of these cations must thus occur by increasing the kinetic barriers of the degradation reactions.

Stability of N-alicyclic QA cations

A fundamental and comprehensive study of the alkaline stability of a large number of QA groups was conducted by Marino and Kreuer in 2015.[11] In the study, the half-life of different cations was measured in 6 M aq. NaOH at 160 °C and the cations were ranked accordingly. A selection is shown in **Figure 9**. *N*-Alicyclic QA groups were found to be exceptionally stable and two piperidine-based cations, *N*,*N*-dimethylpiperidinium (DMP) and 6-azonia-spiro[5.5]undecane (ASU), possessed the highest alkaline stability in the chosen conditions. The results also suggested that placement of otherwise stable cations in benzylic positions severely reduced the alkaline stability, as illustrated in **Figure 9** for benzyl-TMA and benzyl-methylpiperidinium. They also found that benzylic cations that degrade *via* ylid formation may cause radical formation, initiating other type of polymer degradation reactions.[107]

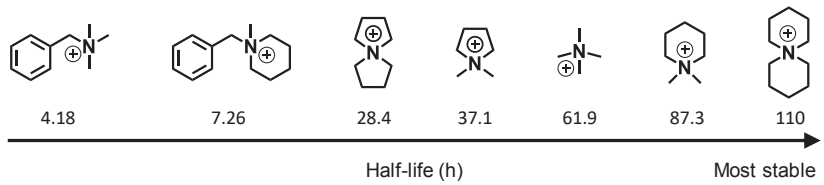

Figure 9. A selection of QA groups investigated by Kreuer et al. arranged according to their established half-life in 6 M aq. NaOH at 160 °C.[11]

The observed high alkaline stability of the *N*-alicyclic QA groups is quite remarkable, especially since each ring has several β-protons available for Hofmann elimination. According to Marino and Kreuer the resistance towards Hofmann ring-opening elimination is ascribed to unfavorable bond angles and bond lengths of the piperidinium ring in the transition states of the this type of degradation reaction (**Figure 8b**).[11, 117] Analysis of the degradation products showed that degradation of the *N*-alicyclic QA cations only occurred *via* ring-opening α-substitution (ASU) or methyl substitution (DMP), as shown in **Figure 10**, with no sign of Hofmann elimination.[11] It was with basis in these findings, ideas for the polymers presented in Paper I – V were developed and realized.

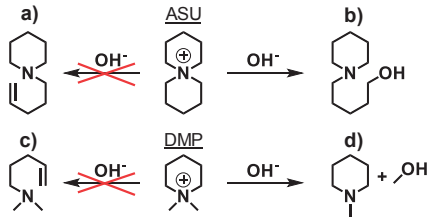

Figure 10. Plausible degradation reactions of the ASU and DMP cations. a) And c) Hofmann ring-opening elimination (E2) and b) and d) nucleophilic substitution (S_N2). Only b) and d) was observed by Marino and Kreuer.[11]

2.2.4 Issues with alkaline stability studies of cationic polymers

A large variety of the different polymer backbones and cations mentioned above have been explored in the process of developing novel and high-performance HEMs for fuel cells. Part of the efforts invested have been focused on the preparation of alkali-stable HEMs. Hence, a lot of structure-property relationships on the subject have been published and it has helped the field to progress.[35, 38, 101] However, interpreting and comparing data from different studies or drawing general conclusions on HEM durability is not straightforward.

One issue with these studies is the sheer number of different methods used to assess the alkaline stability. Common approaches include studying the IEC, ion conductivity and/or the chemical structure as a function of storage time in alkaline solutions, ranging from 1 - 10 M aq. NaOH/KOH at different temperature.[35, 103, 124] This variety makes comparison between different studies difficult and the introduction of a standard procedure for *ex-situ* alkaline stability assessment would simplify the situation.

Another problem involves the study of the alkaline stability of model compounds, which are compounds prepared to mimic the cation in the anticipated polymer.[106] Since the degradation processes of HEMs are complex, it is often difficult to isolate the contribution from different components on the overall degradation, *e.g.* degradation of backbone or cation.[106] By instead studying model compounds data analysis can be simplified.[106] However, because the degradation processes within polymers are *so* complex, an alkali-stable model compound does not directly translate to an alkali-stable HEM. For example, unsuitable placement of an otherwise stable cation might both cause backbone degradation[68], or enable degradation of the cation itself.[125, 126] Hence, the design of a cationic polymer is crucial for its properties and the combination of an alkali-stable backbone and cation must be well thought through in order to avoid the introduction of unforeseen vulnerabilities.

2.3 Approach and aim

The work presented in this thesis was focused on the development of different synthetic strategies to prepare and explore polymers functionalized with *N*-alicyclic cations. With basis in literature and previously gathered knowledge, interesting polymer structures were identified, and synthetic strategies developed and verified. In the lab, these polymers were then realized, and subsequent HEMs were characterized with focus on thermal and alkaline stability, water uptake, ion conductivity and morphology. Additional information was acquired by studying how small structural changes of the prepared polymers affected the aforementioned properties. The obtained structure-property relationships were then added to the pot of knowledge, and the iterative process of developing new ideas was continued. The ultimate goal of this process was to discover and develop an alkali-stable and membrane-forming polymer material in which the inherently high alkaline stability of the *N*-alicyclic QA cation could be fully utilized. Preferably, this polymer should also be prepared using commercially available compounds using high yield and straightforward (short) synthetic procedures. Examples of the different types of polymers synthesized and studied in this thesis are found below in **Figure 11**.

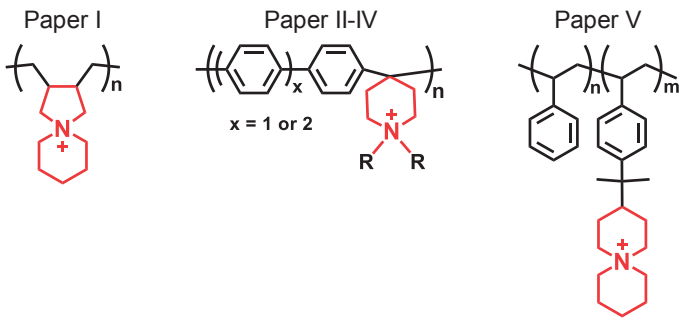

Figure 11. Examples of *N*-alicyclic QA cation functional polymers presented in the included papers.

3 Experimental methods

This section covers the experimental part of the thesis work, with focus on synthesis, analysis and the different materials used.

3.1 Synthesis

3.1.1 Polymerization

Cyclopolymerization

Radical polymerization of various multiallyl QA salts was studied by Butler et al. in the late 1940s and 50s and the results were published as a series of papers.[127-134] At that time, it had been established that radical polymerization of non-conjugated monomers with more than one unsaturation produced crosslinked materials or formed linear polymers carrying unreacted alkenes. The results of the first publication in the series agreed with that, as the studied polymerizations of monomers with at least three unsaturated (allyl) groups produced crosslinked polymers with ions only available for ion-exchange.[127] In later experiments Butler and coworkers found that polymers prepared from diallyl QA salts contained no residual double bonds and were water soluble, indicating that a linear polymer was produced even though both allyl groups were taking part in the polymerization. On top of this, they also found that monoallyl QA salts did not polymerize at all. In the eighth and most cited publication of the series, Butler et al. proposed a mechanism for the formation of linear and water-soluble polymers from diallyl QA salts. The reported mechanism consisted of initiation, intra-molecular cyclization and inter-molecular propagation yielding a polyelectrolyte with repeating units consisting of 6-membered rings.[134] In-depth analysis later revealed that the repeating units were in fact made up of 5-membered rings produced in a slightly different polymerization mechanism, which is shown in **Scheme 1**.[135]

The cyclopolymerization of diallyldimethylammonium chloride (DADMAC or M^+) is typically conducted in water at high monomer concentrations (50 – 70 wt%) with ammonium persulfate (APS) as initiator.[135] The primary radical ($I^\bullet$, **Scheme 1**) is formed either by complex formation of the persulfate ion with monomer cations followed by its decomposition, or by redox reactions between the persulfate ion and the Cl^- ion.[136] $I^\bullet$ and M^+ reacts to form a secondary radical (*ii*) in the initiating step, which is followed by the formation of the 5-membered ring (*iii*) in an intramolecular

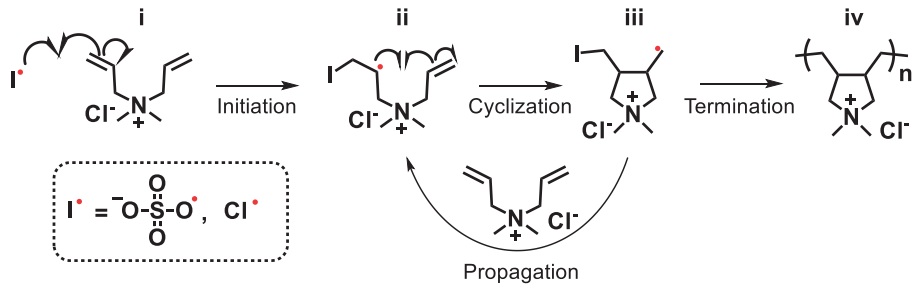

Scheme 1. Mechanism of APS initiated radical polymerization of DADMAC, including initiation, alternating intra- and intermolecular propagation as well as termination. • = radical.

cyclization reaction. A polymer, PolyDADMAC (*iv*), is then produced in a sequence of propagation and cyclization steps, before propagation is terminated. Termination most commonly occurs *via* combination but can also occur by chain degradation reactions with $Cl^{\bullet}$ moieties. Dead chains are also formed by chain transfer to monomer.[136]

This type of cyclopolymerization exhibits some interesting characteristics. For example, the overall polymerization rate is significantly increased at high $[M^+]$ and the ratio $k_p/k_t^{0.5}$ shows a clear increase between 1.5 - 4 mol l^{-1}.[136] A reason for this behavior is that the monomer salt not only acts as a monomer, but also as an electrolyte, which decreases the Coulombic interaction between the propagating chain and M^+. This effect increases with $[M^+]$.[136] The presence of M^+ also speeds up the primary radical formation by complex formation with the persulfate anion.[136]

In an early patent by Butler, it was shown that various diallylammonium salts, such as diallyldimethyl, -pyrrolidinium, -piperidinium and -morpholinium all could be employed to prepare polyDADMAC type polymers.[137] In the same publication, the effect the counterion had on the polymerization was also reported. In polymerizations conducted at the same conditions, monomers in the Cl^- form gave polymers of much higher molar mass than monomers in the Br^- form.[137] No reason was given for this observation, but since the Cl^- ion is involved in both initiation and termination, changing the counterion could probably affect the equilibria of the reactions and, thus, the resulting molar mass.

PolyDADMAC is today mass-produced industrially and used as a flocculating agent in *e.g.* water treatment and paper manufacturing.[138]

In this thesis work cyclopolymerization was used to prepare the water-soluble *N*-spirocyclic polyelectrolytes studied in Paper I.

Polyhydroxyalkylation

The first hydroxyalkylation reaction was reported already in 1872 by A. Baeyer in a study of the condensation of trichloroacetaldehyde and benzene in sulfuric acid.[139] Since then these Friedel-Crafts type reactions, where different carbonyls and electron rich arenes react, have been widely used to produce different industrial chemicals, such as bisphenol A. The field advanced rapidly with the work on superelectrophilic activation by Nobel laureate Olah and coworkers.[140] They showed that the reactivity of certain electrophiles were significantly enhanced in contact with strong Brønsted or Lewis acids (superacids) and called the reactive species formed superelectrophiles.[140] This discovery allowed for high-yield and specific hydroxyalkylations using less reactive arenes[141] and for the preparation of polymers in superacid mediated polycondensations, called polyhydroxyalkylations, pioneered by Zolotukhin et al.[142-144] A range of different carbonyl and non-activated aromatic hydrocarbons compounds, employed as A_2 and B_2 or AB_2 monomers, have been studied and used to prepare high molar mass linear and hyperbranched polymers.[142-147] The polyhydroxyalkylation reaction was quite recently postulated as an effective method to prepare ether-free, high T_g membrane-forming polymers for use as backbones for HEMs,[68, 75] and has been frequently studied for this application since.[74, 76-82, 94, 148, 149]

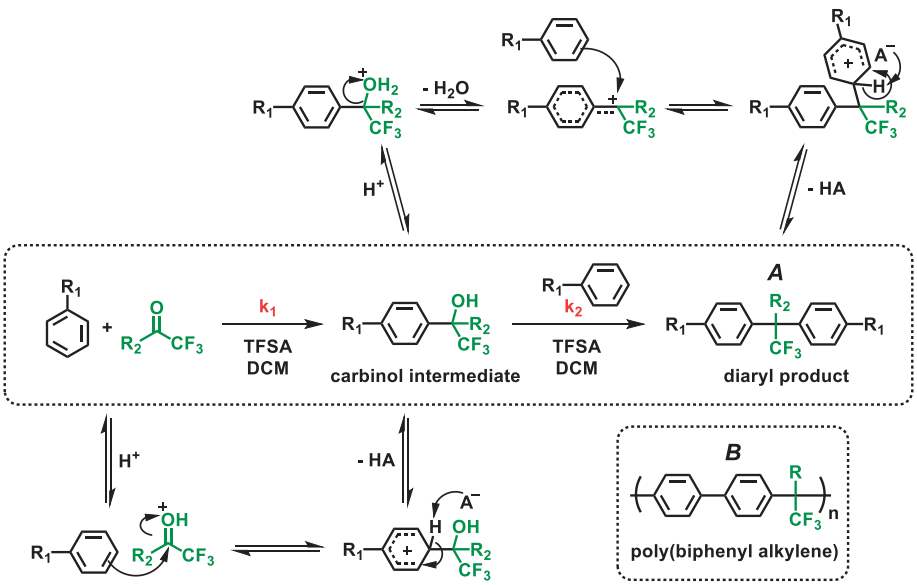

Scheme 2. Hydroxyalkylation of a non-activated arene with a trifluoroketone in TFSA and DCM, with included reaction mechanisms. k_1 and k_2 are rate constants.

An example of a superacid mediated hydroxyalkylation reaction is shown in **Scheme 2**. Here a trifluoroketone and an arene reacts in two steps to form a diaryl product (***A***) in a solution of trifluoromethanesulfonic acid (TFSA) and dichloromethane (DCM). Each step has been assigned its own rate constant (k_n). In the first step, the protonated trifluoroketone, an electrophile with enhanced reactivity, reacts with an arene to form a carbinol intermediate. Subsequently, a tertiary carbocation is formed, which condenses with a second arene forming the product. The reaction mechanism is also included in **Scheme 2**. By using an A_2 monomer, i.e. biphenyl (R_1 = Ph), as the arene reactant, a poly(arylene alkylene) (PAA) (***B***) can be produced.

The rate constants (k_1 and k_2, **Scheme 2**) of a hydroxyalkylation reaction depend strongly on the compounds used and the employed reaction conditions. Thus, the ratio between the rate constants (k_1/k_2) can be tuned by reaction design.[150] For example, the ratio for the reaction between 1,1,1-trifluoroacetone and anisole in TFSA is 350 ($k_1 > k_2$), while with benzene as nucleophile the ratio is 10^{-4} ($k_1 << k_2$).[150] The ratio can also be controlled by changing the acidity of the reaction solution. With increasing acidity, k_1 decreases and k_2 stays intact so the ratio (k_1/k_2) decreases.[150] Together these characteristics mean that by careful reaction design either a mono- or a diarylated product can be obtained. On top of this, if $k_1 < k_2$, the first step will be rate determining and polyhydroxyalkylation reactions governed by such characteristics may be accelerated by non-stoichiometric conditions, which is unusual for polycondensation reactions. With the carbonyl compound in excess, the polymerization rate will increase with increasing molar imbalance between the monomers.[150] Zolotukhin et al. showed that only a 15-20% excess dramatically increase the reaction rate and these polymerizations were completed within minutes. However, a too large molar excess of the carbonyl compound led to side reactions and crosslinking.[150]

Another type of carbonyl compound that has been used in superacid mediated polyhydroxyalkylation reactions, in addition to trifluoroketones, is piperidones.[145, 151] Piperidone was first indicated as a candidate for superelectrophilic activation in an electrostatic field effect study related to different oxocarbenium ions.[152] In a later study by Klumpp et al., different piperidones were diarylated in good to excellent yields (80 – 99%) in TFSA/DCM mixtures.[151] The highest yields were obtained with *N*-substituted 4-piperidones. By reacting mono- or diphenylated piperidone with chlorobenzene it was also shown that at least one of the electrophilic aromatic substitutions was reversible, as can be seen in **Scheme 3**. Both reactions gave a mixture of three products, consisting of piperidones functionalized with either diphenyl, diphenylchloride or monophenyl and monophenylchloride.[151]

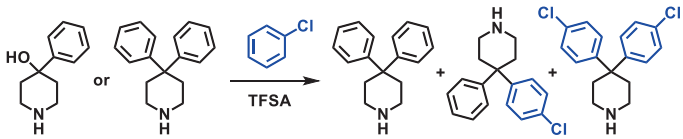

Scheme 3. Reactions of mono- and diarylated piperidones with chlorobenzene undertaken by Klumpp et al. showing that hydroxyalkylation reactions with piperidone are equilibrium reactions.[151]

Piperidones have also been used to prepare both linear and hyperbranched polymers of high molar mass by condensation with *e.g.* biphenyl and terphenyl.[145] This is especially interesting for HEM research, since it enables a quick route to rigid aryl ether-free and membrane forming polymers carrying secondary or tertiary piperidine moieties. A typical polymerization of *N*-methyl piperidone (mPip) and *p*-terphenyl in TFSA, trifluoroacetic acid (TFA) and DCM is shown in **Scheme 4a**. In this thesis work, different arene and piperidone monomers have been used to prepare a variety of poly(arylene piperidine)s in polyhydroxyalkylation reactions (Paper II-IV), which were developed based on the procedures presented by Cruz et al.[145]

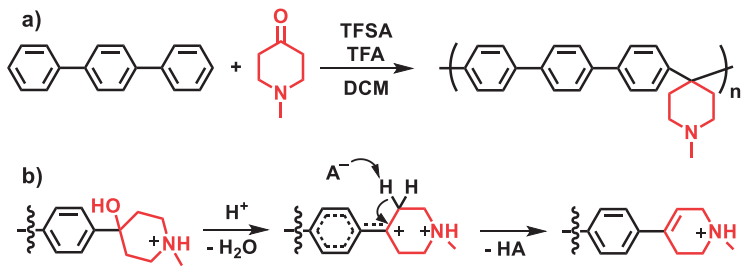

Scheme 4. a) Polyhydroxyalkylation of p-terphenyl and mPip. b) E1 reaction during polyhydroxyalkylation forming an irreversible chain end.

An unexpected challenge arose during our work with polyhydroxyalkylation reactions involving piperidones. It was noticed that the viscosity of the reaction solution reached a maximum during the reaction and suddenly started to decrease. ^{1}H NMR analysis of samples taken from the polymerization reaction after different times indicated that a side reaction competed with the propagation reaction. An emerging signal at 6.3 ppm seemed to be correlated to the decrease of the reaction solution viscosity. No information about this side reaction was found in literature, but the signal shift indicated that it originated from an alkene, which most probably was formed in an irreversible E1 reaction, as shown in **Scheme 4b**.[80] Since the propagation in this type of polymerization is an equilibrium reaction, the accumulation of these dead chain ends not only terminate further growth but also lead to a decrease of the molar mass of already formed polymer strands. Hence, explaining

the observed decrease of the reaction solution viscosity over time. In order to mitigate the elimination issue, polymerizations were conducted at 0 °C and the reactions were stopped when viscosity reached its maximum.

3.1.2 Polymer modification and functionalization

Hydroxyalkylation of polystyrene

The hydroxyalkylation reaction can also be used to modify aromatic polymers with various functional groups.[153] For example, polystyrene can be functionalized using tertiary alcohol reagents in triflic acid.[153] In this reaction, the aromatic ring of the polystyrene (PS) couples to a tertiary carbocation formed after protonation of the tertiary alcohol reagent.

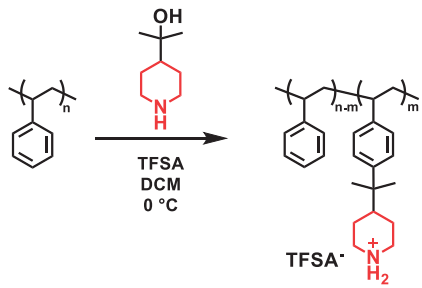

Scheme 5. Functionalization of PS with a tertiary alcohol reagent in a triflic acid mediated hydroxyalkylation reaction.

In Paper V, PS was tethered with 2-(piperidine-4-yl)propane-2-ol (Pip*t*OH) as shown in **Scheme 5**. This reaction proceeded as a two-phase suspension, because of low solubility of PS in the reaction solution. With time, the suspension became more homogeneous, probably due to the gradual dissolution of functionalized polymer. Using this method, PS could be functionalized up to 30% and attempts to reach higher degrees of functionalization rendered insoluble products. The secondary amines in the functionalized PS were readily available for subsequent quaternization.

Quaternization

Charges, in the form of QA cations, were introduced by quaternization of amines already present in precursor polymers. The amines were quaternized in S_N2 reactions with alkyl halides undertaken in aprotic polar solvents, typically DMSO, NMP or a mixture of both.[116] Tertiary amines were transformed to QA groups in Menshutkin reactions without addition of any catalyst (**Scheme 6a**). Some quaternization reactions of tertiary amines and all quaternizations of secondary amines were conducted in the presence of a base (**Scheme 6b**). Depending on the alkyl halide,

either *N*,*N*-diisopropylethylamine (DIPEA) or K_2CO_3/$CaCO_3$ was used as a base. Because iodomethane is small enough to react with DIPEA, despite the bulkiness of the base, one of the carbonates had to be used for these reactions. The reactivity of the alkyl halide also influenced the choice of reaction temperature. All quaternizations with iodomethane were performed in the dark at ambient conditions, while reactions involving alkyl bromides were heated to ~80 °C.

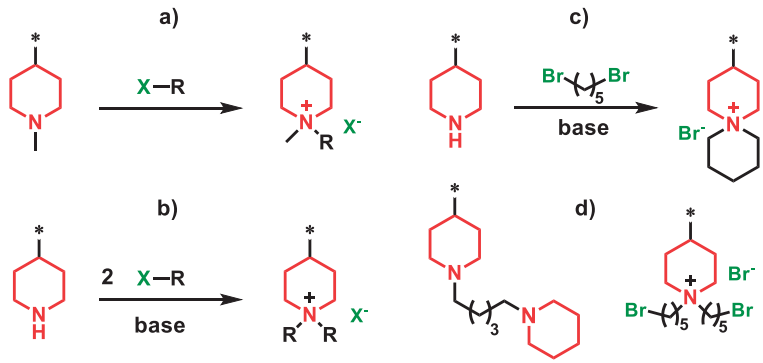

Scheme 6. Different quaternization reactions of piperidine moieties with alkyl halides. a) Tertiary *N*-methyl piperidine, b) secondary piperidine, c) cycloquaternization of piperidine with 1,6-dibromohexane and d) possible unwanted products from side-reactions in the cycloquaternization.

The term *cycloquaternization* has been frequently used during this thesis work and refers to the preparation of *N*-spirocyclic QA cations from secondary mono-cyclic amines by reaction with *α*,*ω* -dibromoalkanes as shown in **Scheme 6c**. The functionalization reactions occur in two distinctly different steps. First, a tertiary amine is formed in an intermolecular substitution reaction between a secondary amine and a dibromoalkane. This is followed quickly by an intramolecular ring-closing substitution reaction. Unwanted products, shown in **Scheme 6d**, formed in side reactions were avoided by maintaining a low reactant and polymer concentration, in addition to adding the electrophile and base dropwise to the reaction solution. These precautions decreased the rate of all intermolecular reactions, while the rate of the intramolecular reactions was left unaffected, thus, decreasing the risk of crosslinking.

Another important aspect to avoid crosslinking was to maintain a homogeneous solution throughout the reaction. Any inhomogeneity, *e.g.* precipitation, leads to a locally increased polymer concentration and an increased risk of crosslinking. Therefore, solvents or solvent mixtures were carefully chosen for each different cycloquaternization reaction. In contrast, quaternization of poly(arylene piperidine)

with iodomethane always proceeded to full conversion without observable side reactions even though the precursor polymer was insoluble in the chosen solvent.

Crosslinking and subsequent quaternization

A method utilized in this work to control the water uptake was crosslinking. By introducing crosslinks, different polymer strands become covalently connected to each other and their relative movement limited, thus decreasing the ability of the HEM to swell and its water uptake. In Paper IV, crosslinks were introduced during a reactive casting step, in which a precursor polymer with pendant tertiary amines was cast in the presence of a small amount of 1,8-dibromooctane. During casting, the piperidine moieties displace the bromine atoms of the crosslinking agent and quaternized piperidinium units, connected by octyl chains, are formed. The length of flexible alkyl chains was chosen so that the intermediate films would not be too brittle and make them easier to handle. The degree of crosslinking was determined by Mohr titration of the intermediate films. Finally, the IEC of the finished crosslinked HEMs was varied by quaternizing part of the residual tertiary amines using a stoichiometric shortage of iodomethane in water.

3.1.3 Monomer synthesis

Only one project involving monomer synthesis is included in this thesis and that is the synthesis of *N,N*-diallylazacycloalkane quaternary ammonium bromide and chloride salts used in Paper I.

Starting with different heterocyclic amines, four different *N,N*-diallylammonium salts were prepared in a two-step synthesis based on the procedures presented in a paper by de Vynck et al.[154] In theory to monomers could be prepared in one step, but in order to avoid a tedious purification process, including the separation of different water soluble salts, a perhaps slower but simpler route was chosen. First, a secondary amine was reacted with allyl bromide to form the intermediate *N*-allylamine. After distillation, the monomer, *N,N*-diallylammonium bromide or chloride, was prepared from *N*-allylamine in a reaction with allyl bromide or allyl chloride, respectively. Due to the different reactivity of the allyl halide reagents, the second step was performed either in diethyl ether at room temperature or in NMP at 75 °C. The precipitated monomer salt was washed several times with diethyl ether and used in subsequent cyclopolymerizations without further purification.

3.1.4 Membrane preparation

All films and HEMs included in this thesis work were prepared by solvent casting from 5 wt% polymer solutions placed in Petri dishes (Ø = 5 cm). The solutions,

prepared with DMSO or NMP, were filtered using a Teflon syringe filter (Millex LS, 5 µm) prior to casting in a well-ventilated oven at 70 – 85 °C during at least 48 h. The obtained membranes were 50 – 100 µm thick and were stored in water at least 48 h before any measurements.

Blending

An efficient strategy to improve mechanical properties, mitigate swelling and decrease water uptake of an HEM is by preparation of blend membranes. By blending a cationic and an anionic polymer, strong interactions in the form of ionic complexes arise between the polymers. These complexes lower water uptake by both decreasing the effective IEC and working as crosslinks that limit the swelling.

In this thesis work, blending was used to improve the properties of PS HEMs. Cationic PS was co-cast with polybenzimidazole (PBI-O) from DMSO solutions to form homogeneous blend HEMs. These were then treated with 1 M aq. NaOH to deprotonate part of the –NH– groups of the PBI-O component and form piperidinium-imidazolate complexes as shown in **Figure 12**. These complexes work as ionic crosslinks between the two polymer components and are stable as long as the blend HEMs are kept under alkaline conditions. Hence, all blend HEMs were stored in alkaline solution prior to and between all measurements. Since the blend HEMs had to kept in alkaline solution, their IECs could not be determined using Mohr's or acid-base titration methods.

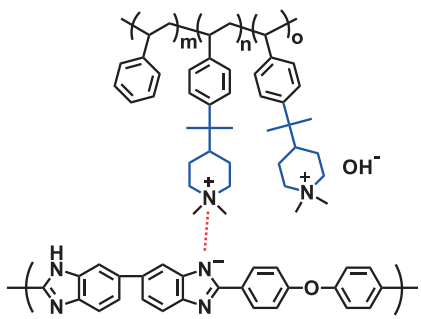

Figure 12. A piperidinium-imidazolate complex acting as a crosslink in a blend between functionalized PS and polybenzimidazole (PBI-O).

3.2 Characterization methods

3.2.1 Polymer characterization

Differential scanning calorimetry (DSC)

The glass transition temperature (T_g) of different polymer samples was determined by studying the heat flow to the sample at 10 °C min^{-1} using a Q2000 DSC (TA Instruments). All samples were analyzed in two heating cycles to remove any thermal history and the T_g was taken at the inflexion point in the thermogram during the second cycle. Due to the quick absorption of water from the air into an HEM, the glass transition region can often be broadened, which makes it difficult to distinguish. Therefore, non-quaternized precursor polymers were typically studied instead.

Viscosity measurements

Solubility and instrument limitations made it impossible to study the molar mass of the synthesized polymers by gel permeation chromatography (GPC). The precursor polymers (PAA-type) prepared for papers II-IV were soluble in chloroform when neutral and analysis with GPC was attempted several times. However, no elution time could be determined because no signal was detected. This was most probably caused by polymer adsorption to the columns. Therefore, to estimate or get an indication of the molar mass, the intrinsic viscosity of dilute polymer solutions in water (Paper I) or DMSO (Paper II-IV) was measured using an Ubbelohde viscometer.[155] To prevent the polyelectrolyte effect, NaCl (1 M) was added to the water and LiBr (0.1 M) to the DMSO solutions. A water bath was used to keep the temperature constant during the measurements. The elution times for the sample solutions of different concentrations (t_s) was compared to the elution time of the solvent (blank, t_b) and the reduced (η_{red}) and inherent viscosity (η_{inh}) was calculated using the following equations,

$$\eta_{red} = \frac{\frac{t_s}{t_b} - 1}{c} \quad (1)$$

$$\eta_{inh} = \frac{\ln\left(\frac{t_s}{t_b}\right)}{c}, \quad (2)$$

where c is the polymer concentration. The intrinsic viscosity [η] was taken as the average intersection of η_{red} and η_{inh} with the y-axis.

Nuclear magnetic resonance (NMR) spectroscopy

NMR spectroscopy was used to study and verify the molecular structures of synthesized monomers and polymers. On a Bruker DRX400 spectrometer, ^{1}H and ^{13}C NMR spectra were obtained at 400 and 100 MHz, respectively. Solvents used for the analysis include DMSO-d_6 (δ = 2.50 ppm), D_2O (δ = 4.79 ppm) and chloroform-d (δ = 7.26 ppm).

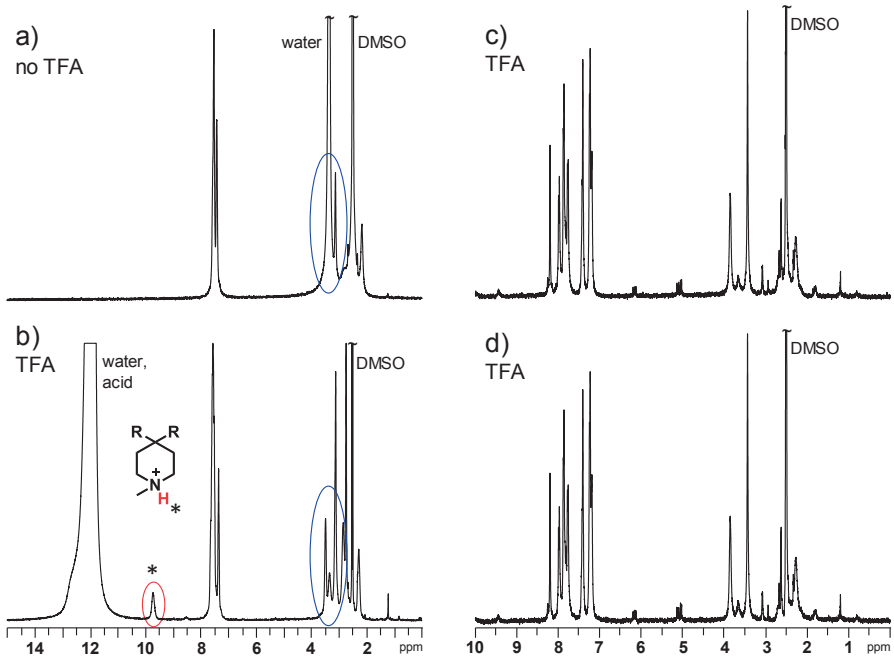

Figure 13. ^{1}H NMR spectra before (a) and after (b) the addition of TFA to a sample solution. Protonation caused both a shift of the water signal revealing previously hidden signals (blue oval) as well as tertiary amines (red oval). Spectra (c, d) were both taken one month apart of the same sample solution, with added TFA, to demonstrate that no proton-deuterium exchange occurs with time.

In many cases, when NMR analysis was conducted with DMSO-d_6 as the solvent, 1,1,1-trifluoroacetic acid (TFA) was added to the solution. It was discovered, by chance, that residual acid left from the polymerization of PAAs could be very useful for NMR analysis. It not only protonated tertiary amines, but also the water molecules, shifting the water signal to above 10 ppm, as shown in **Figure 13a-b**. Thereafter, TFA was systematically used to uncover otherwise hidden signals and to reveal tertiary amines, which in the protonated form gave rise to their own signal (R_3-N^+-*H*, **Figure 13b**). The latter became especially important during the study of polymer and HEM degradation in alkaline media. Since all (common) degradation mechanisms involving *N*-alicyclic cations lead to the formation of tertiary amines

covalently attached to the polymer, being able to quantify the amount of tertiary amine formed is a very useful tool. However, to ensure the credibility of the data, it is crucial to verify that no proton-deuterium exchange occurs over time. This would change the signal intensity and integral, making the method useless. However, as can be seen in **Figure 13c-d**, which display two NMR spectra of the same sample solution taken more than 1 month apart, no observable changes occurred with time.

3.2.2 Membrane characterization

Titration and water uptake

One of the fundamental properties of an HEM, which affects both the water uptake and ion conductivity, is the number of charges per gram of polymer, the ion-exchange capacity (IEC). It is usually expressed in mmol g^{-1} or milliequivalents (meq.) g^{-1} and represents the number of ions available for ion-exchange in the polymer. Because OH^- ions form carbonates in contact with the CO_2 in air, the IEC in OH^- form (IEC_{OH}) of the HEMs was not determined directly *via* acid-base titrations. Instead, it was calculated from IEC_{Br} obtained from Mohr titrations, which were carried out as following. Approximately 0.05 g of an HEM sample in Br^- form was dried in a vacuum oven (50 °C) and weighed, then ion-exchanged in 0.2 M aq. $NaNO_3$ for at least 48 h. Subsequently, the exchanged Br^- ions were titrated with 0.01 M aq. $AgNO_3$ using $KMnO_4$ as colorimetric indicator. Each titration was conducted four times in order to eliminate random errors.

The water uptake after storage at different temperatures (20 – 80 °C) was determined by comparing the dry sample weight and the weight after immersion (W'_{OH}). However, due to issues with drying the membrane in OH^- form (degradation), the dry weight in OH^- form (W_{OH}) was calculated from W_{Br} using the IEC. In order to avoid formation of carbonates during the water uptake studies, all ion-exchange and immersion procedures were undertaken in a CO_2-free nitrogen environment (desiccator).

$$WU = \frac{W'_{OH}}{W_{OH}} \tag{3}$$

Thermogravimetric analysis (TGA)

The thermal stability of HEM samples and precursor polymers was studied at a heating rate of 10 °C min^{-1} under N_2 on a TGA Q500 (TA instruments). Samples were pretreated at 110 - 120 °C for at least 10 min to remove residual water and solvents,

before studying weight changes during heating from 50 to 600 °C. The decomposition temperature ($T_{d,95}$) was defined as the temperature at 5% weight loss.

Alkaline stability studies

In order to assess the *ex-situ* chemical resistance of an HEM under alkaline conditions at elevated temperature (alkaline stability), changes of different membrane properties such as ion conductivity, water uptake, IEC and/or molecular structure are typically studied as a function of storage time.[35, 156-159] In this work, ^{1}H NMR spectroscopy was the method of choice because it allowed for quantitative as well as qualitative assessment of the degradation. As long as the membrane samples remained soluble after alkaline treatment, NMR analysis can provide valuable information left out by the other methods, *i.e.* about degradation mechanisms.

Figure 14. Sample holders used to store samples in alkaline media for alkaline stability assessment at >80 °C. Left: pressure safe glass container with screw cap and a special made Teflon insert. Right: Assembled holders in an oven.

The stability assessment was conducted by immersing membrane pieces (~15 mg) in alkaline solution at elevated temperature (90 – 120 °C) for a certain time. In order to avoid water evaporation, glass breakage due to high pressure and unnecessary carbonate formation during the testing, samples were placed in heavy-wall pressure glass tubes with screw caps equipped with custom-made Teflon inserts (**Figure 14**). These were then placed in an oven set to the desired temperature, which was monitored with a laboratory thermometer. After storage at a fixed temperature in alkaline solution, the sample pieces were taken out at regular intervals to be ion-exchanged to the Br^- form, thoroughly washed and dried (50 °C, vacuum) before NMR analysis.

In Paper I, deuterated alkaline solutions (2 M KOD/D_2O) of the different polyelectrolytes (7 wt%) were studied by NMR spectroscopy after different storage

times at 90 and 120 °C. Prior to analysis, the extracted samples were diluted to 1 M KOD/D_2O in order to decrease shimming issues in the instrument. In one case, the alkaline stability of a polyelectrolyte sample was studied under accelerated conditions by using 2 M KOD in CD_3OD/D_2O at 90 °C. The solution was prepared by diluting 1 g of 40 wt% KOD in D_2O to 3.5 ml using CD_3OD.

Electrochemical impedance spectroscopy (EIS)

All ionic conductivity measurements were performed under fully hydrated (immersed) conditions by EIS on a Novocontrol high resolution dielectric analyzer V 1.01S. The in-plane resistance of sample pieces (14 × 14 mm, ~50-70 µm thick) placed in a sealed two probe cell was determined at different temperatures using an AC voltage with an amplitude of 50 mV at 10^7 - 10^0 Hz.

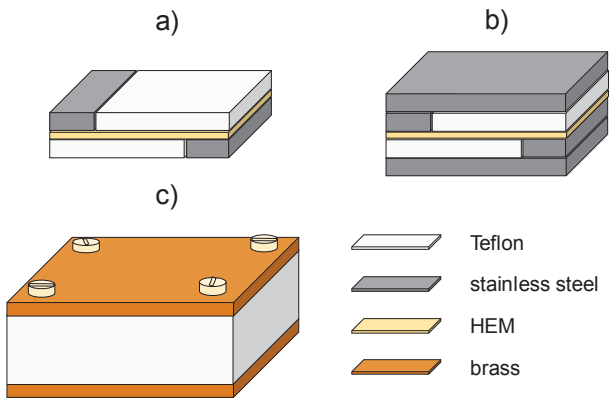

Figure 15. The two-probe cell used for in-plane impedance spectroscopy measurements of HEMs under fully hydrated (immersed) conditions. a) An HEM sandwiched between two stainless steel electrodes and two Teflon spacers, b) additional stainless steel plates for improved contacting and c) the assembled and closed cell with top and bottom made of brass.

The cell configuration and assembly are shown in **Figure 15a-c**. First, the HEM is sandwiched between two stainless steel electrodes and two insulating Teflon spacers (a). Two additional stainless steel plates (b) are placed above and below, and the whole stack is placed in a Teflon cell and closed with brass plates (c). To avoid surface conductivity and because of instrument configuration, the electrodes are positioned on opposite faces of the membrane and the cell is contacted on top and bottom. The assembly was undertaken quickly (<30s) in order to limit contamination by CO_2 and once the cell has been sealed, the hydration level is maintained. With this method, as long as the thickness of the membrane is carefully determined, the measured ionic conductivity should never be erroneously high. However, due to possible CO_2 contamination during ion-exchange, washing and cell assembly, it

might be too low. Thus, in general two measurements for each type of HEM was conducted to ensure the accuracy of the obtained value.

From the measured bulk resistance (R) at different frequencies, the conductivity of the membrane (σ) was calculated by the instrument using the following equation:

$$\sigma = \frac{L}{A \times R} \tag{4}$$

where L is the distance between the electrodes and A is right-angle cross-sectional area of the membrane. Subsequently, the bulk ionic conductivity is taken as the plateau value in a plot of σ' as a function of the frequency (**Figure 16**).

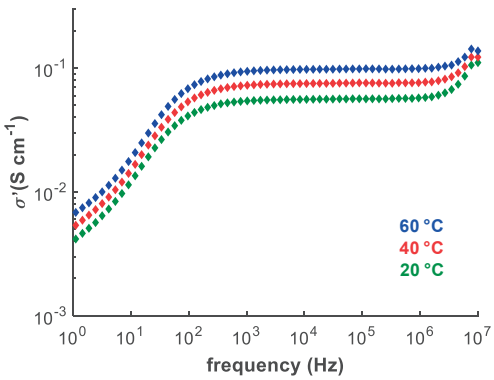

Figure 16. Conductivity data as a function of frequency measured at 20, 40 and 60 °C, corresponding to ionic conductivity of 56, 75 and 98 mS cm^{-1}, respectively, obtained from the plateau.

Small Angle X-ray Scattering (SAXS)

SAXS is a technique in which the morphology (phase separation) of a material is studied by illumination with collimated monochromatic X-rays of a well-defined wave vector (k_i). The incident electromagnetic waves cause the electrons in the sample to oscillate and emit spherical waves of the same frequency and energy as the incoming radiation (wave vector k_s). The scattered X-rays will interfere with each other and their intensities are collected by a detector as a function of their scattering angle (2θ) as shown in **Figure 17**. The measured intensity is typically plotted as a function of the magnitude of the scattering vector, q, which is the difference between the wave vectors k_i and k_s and is related to the scattering angle by:

$$q = |\bar{k}_i - \bar{k}_s| = \frac{4\pi \sin(\theta)}{w} \tag{5}$$

where w is the wavelength of the incident radiation.

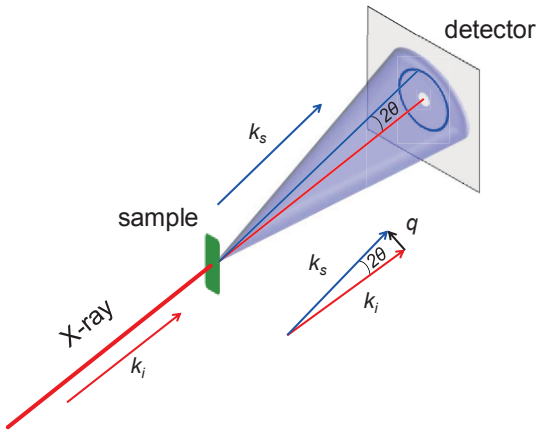

Figure 17. Schematic of the beam path in a SAXS measurement with scattering angle, wave vectors and scattering vector (q) displayed.

The presence of intensity maxima observed by the detector indicate that there are ordered/periodic structures in the studied sample which cause constructive interference at certain scattering angles. The scattering vector of an intensity maximum (q_{max}) is related to a certain characteristic separation distance (d) of the features in the sample responsible for the scattering. Using Eq. 5 and Bragg's law this distance is calculated as:

$$d = \frac{2\pi}{q_{max}} \quad (6).$$

A scattering profile of an HEM with an ordered morphology is shown in **Figure 18**. The scattering maximum observed at 1.2 nm^{-1} is a so called ionomer peak, which is a typical feature of polymers carrying charges and was first studied by Longworth et al.[160] Their studies showed that the scattering profile of poly(ethylene-methacrylic acid) did not change with temperature, but the intensity of the ionomer peak did decrease if the sample was allowed to take up water. Thus, it was believed that the scattering was caused by a phase separated but molecularly connected ionic phase within the polymer matrix.[160] Since this discovery, the presence of a well-defined morphology of ionic clusters, observed by SAXS, within PEM and HEMs have been correlated to high ionic conductivities, as discussed in the part covering morphology in the introduction section.[161] The characteristic separation distance (d) calculated from SAXS data of HEMs is correlated to the average distance between these clusters and is affected by the molecular structure and properties of the polymer chain.[161] This

includes the hydrophilicity of the cation[88], length of alkyl chains connected to the cation[56, 57] and rigidity of the backbone[74].

A SAXSLAB SAXS Instrument from JJ X-ray A/S, Denmark was used to gather all the SAXS data presented in this thesis. All SAXS measurements were conducted by Peter Holmqvist and data were collected in a q-range of 0.12 – 8.0 nm^{-1} using Cu K_α radiation (λ = 0.1542 nm).

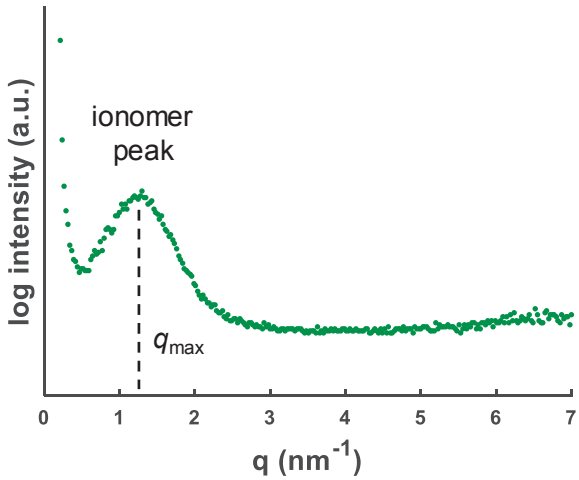

Figure 18. Scattering profile of an HEM with a clear phase separation in the form of ionic clusters. The ionomer peak (q_{max} at 1.2 nm^{-1}) corresponds to features in the membrane with a characteristic separation distance around 5.2 nm.

4 Summary of appended papers

4.1 *N*-spirocyclic polyelectrolytes (Paper I)

In the first paper presented in this thesis work, the structure-property relationships of four different water soluble *N*-spirocyclic polyelectrolytes prepared by cyclopolymerizations of *N*,*N*-diallylammonium monomers (diallylazacycloalkanes) were studied. The work was focused on studying how the ring size and presence of additional heteroatoms affected the thermal and alkaline stability of these polyelectrolytes. In addition, crosslinked HEMs consisting of PPO and poly(*N*,*N*-diallylpiperidinium chloride) was prepared by reactive membrane casting to demonstrate how to employ these water soluble polyelectrolytes as cationic moieties for membrane use.

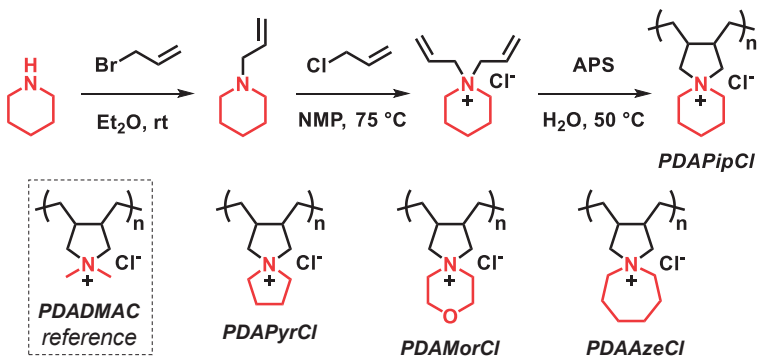

Scheme 7. Synthesis of poly(*N*,*N*-diallylpiperidinium), including the two-step monomer synthesis *via* *N*-allylpiperidine to *N*,*N*-diallylpiperidinium chloride (top). The molecular structures of the other polyelectrolytes presented in Paper I (bottom).

Monomer and polymer synthesis

The procedure for both monomer and polymer synthesis, shown in **Scheme 7**, was strongly inspired by a paper by De Vynck[154], and allowed for a direct and facile preparation of *N*-spirocyclic polyelectrolytes from inexpensive and commercially available starting materials and reagents. The structure of the cations was varied by using different secondary amines as starting material in the monomer synthesis. Starting from pyrrolidine, piperidine, azepane and morpholine, respectively, four different *N*,*N*-diallylammonium monomers were synthesized in two subsequent allylation reactions (**Scheme 7**). These were then employed at high concentrations (60 – 70 wt% in water) in APS initiated cyclopolymerizations during ~20 h at 50 °C.

The obtained polyelectrolytes were named poly(*N*,*N*-diallylammonium *counterion)* and denoted PDA*XY*, where the three letter abbreviation of the ammonium moiety (*X*) and counterion (*Y*) vary between the samples. For example, the polymer made from *N*,*N*-diallylpyrrolidinium bromide was called poly(*N*,*N*-diallylpyrrolidinium bromide) and shortened PDAPyrBr.

To assess the effect of the *N*-spirocyclic structure, the prepared polyelectrolytes were not only compared to each other but also to a commercially available monocyclic polyDADMAC (PDADMAC) reference material (**Scheme 7**).

At first, all monomers were prepared in the bromide form, following the procedure by De Vynck[154], but polymerization of these monomers only resulted in low molar mass polymers (oligomers) with several small ^{1}H NMR signals from impurities of unknown origin. After a brief literature study, a relevant patent was found[137] and the problem was solved by preparing and polymerizing the monomers in the chloride form instead. The molar mass (M_v) of the polyelectrolytes were calculated using intrinsic viscosity data obtained with dilute solution viscometry and Mark Houwink constants found in literature to be between 26 and 61 kg mol^{-1} **(Table 1**).

Table 1. Properties of the polyelectrolytes.

sample	IEC [a] /meq. g^{-1}	[η] [b] /dl g^{-1}	M_v [c] /kg mol^{-1}	$T_{d,95}$ /°C
PDADMAC	6.98	0.16	17	263
PDAPyrCl	5.91	0.43	59	336
PDAPipCl	5.46	0.22	26	318
PDAAzeCl	5.07	0.37	49	263
PDAMorCl	5.40	0.44	61	218

[a] Theoretical IEC in OH^- form. [b] Measured in 1 M aq. NaCl solutions at 30 °C. [c] Calculated using the Mark-Houwink equation with literature constants obtained for PDADMAC solutions in 1 M aq. NaCl at 30 °C.[162]

Characterization

The thermal decomposition of the polyelectrolytes under a nitrogen environment was studied by TGA. A clear trend with ring size was observed as the decomposition temperature ($T_{d,95}$) decreased with increasing ring-size: PDAPyrCl > PDAPipCl > PDAAzeCl (**Table 1**). However, comparison of the $T_{d,95}$ of the two 6-ring polyelectrolytes, PDAMorCl (218 °C) and PDAPipCl (318 °C), indicated that the inductive effect of the oxygen atom in PDAMorCl had a severe destabilizing effect, which trumped the effect of the ring size. PDADMAC, the benchmark non-spirocyclic polyelectrolyte, ranked in the middle with the same $T_{d,95}$ as PDAAzeCl, but was outperformed by PDAPyrCl and PDAPipCl. To put these results into context,

the $T_{d,95}$ of PPO functionalized with standard benzyl-TMA and alkyl-TMA cations was observed at 199 and 213 °C, respectively.[57] Hence, the measured thermal stability of both PDAPyrCl and PDAPipCl is very high.

In order to assess the alkaline stability and investigate the active degradation mechanisms, structural changes of the polyelectrolytes dissolved in 2 M KOD/D_2O were monitored by ^{1}H NMR spectroscopy as a function of storage time at 90 or 120 °C. Before analysis, extracted sample solutions were diluted to 1 M KOD/D_2O to decrease shimming issues in the NMR instrument. After storage at 90 °C during 14 days, no significant changes in the spectra of PDADMAC, PDAPyrCl and PDAPipCl could be observed, while both PDAMorCl and PDAAzeCl exhibited signs of degradation. To increase the degradation rate and be able to rank the polyelectrolytes based on their alkaline stability, the storage temperature was increased to 120 °C. The resulting ^{1}H NMR spectra can be found in **Figure 19a-e**. To better illustrate the arising changes, the spectra were overlaid and normalized with respect to the downfield *b* signal. Under these conditions all polyelectrolytes showed signs of degradation and their relative alkaline stability was: PDAPipCl > PDAPyrCl > PDADMAC >> PDAAzeCl > PDAMorCl. Notably, only minor changes were observed for PDAPipCl, indicating a remarkable stability under these harsh conditions. The two least stable samples, PDAAzeCl and PDAMorCl, degraded quickly at 120 °C and both polyelectrolytes precipitated within a few days, most probably due to the decreased water solubility from the loss of ions. PDADMAC, the monocyclic reference, placed in the middle, indicating that employing *N*-spirocyclic cations can be either advantageous or detrimental to the alkaline stability. This depends on the design of the ring structure. An *N*-spirocyclic polyelectrolyte with high alkaline stability should have a low ring strain (6-membered best) and lack unnecessary electron withdrawing heteroatoms, agreeing with previous studies on the degradation of heterocyclic QA salts.[163-166]

By studying and comparing the ^{1}H NMR spectra before and after storage of the polyelectrolytes at 120 °C, shown **Figure 19a-e**, some of the active degradation mechanisms could be elucidated (expanded spectra can be found in the SI of Paper I). For example, the distinctive signals emerging at 4.5 – 6.5 ppm corresponded well with alkene protons. These signals were observed only for PDAAzeCl and PDAMorCl (**Figure 19d-e**), at both 90 and 120 °C and strongly indicated ring-opening of the pendant (red-colored) ring *via* elimination reactions (**Figure 19f**). The lack of these signals for PDADMAC, PDAPyrCl and PDAPipCl indicated that degradation most probably occurred solely *via* substitution reactions. As shown in **Figure 19f**, this type of reaction causes ring-opening of any of the rings or leads to

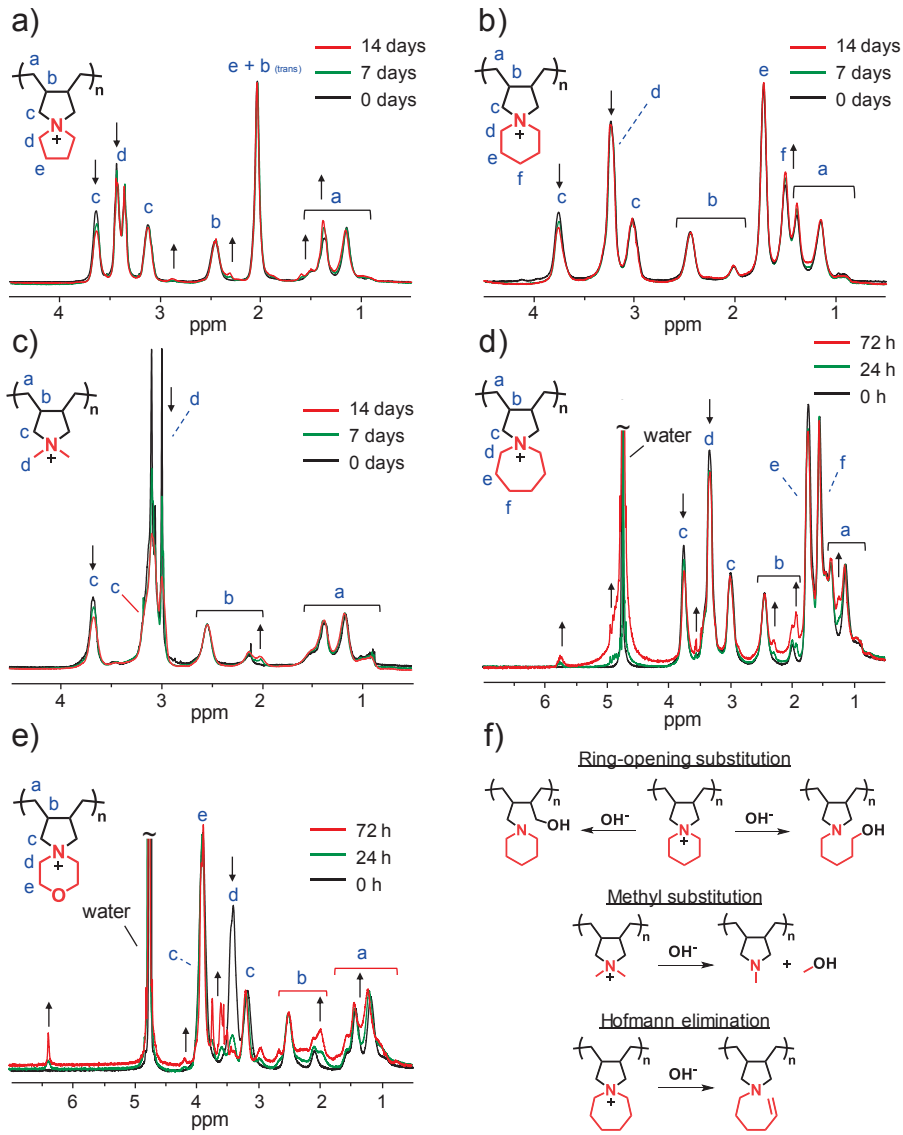

Figure 19. ^{1}H NMR spectra of the polyelectrolytes after different storage times in 2 M KOD/D_2O solutions at 120 °C: a) PDAPyrCl, b) PDAPipCl, c) PDAMorCl, d) PDAAzeCl and e) PDAMorCl. The spectra are normalized with respect to the downfield b signal and the arrows denote changes over time. f) Four plausible degradation mechanisms of the polyelectrolytes.

loss of a methyl group, in the case of PDADMAC. Small emerging signals from products, *e.g.* –CH_2OH, formed in substitution reactions were expected to overlap with the broad polymer signals and be difficult to distinguish. However, the emerging signals at 3.5 ppm observed for the significantly degraded PDAAzeCl and

PDAMorCl were most likely examples of such signals. Similar signals for PDADMAC, PDAPyrCl and PDAPipCl could not, with certainty, be distinguished. Yet, because of the observed difference in the NMR spectra of these three samples, degradation presumably did not occur in the ring closest to the backbone (5-ring).

HEM preparation

In order to prepare HEMs, where the excellent thermal and alkaline stability of the cationic moieties of PDAPipCl can be utilized, the water solubility of the polyelectrolyte must be overcome. Herein, this was achieved by immobilization of the ionic polymer strands in a reactive casting procedure, during which *N*,*N*-diallylpiperidinium chloride was incorporated into PPO. As shown in **Scheme 8**, diallylmethyl QA groups tethered to PPO were copolymerized with *N*,*N*-diallylpiperidinium chloride to form water insoluble HEMs grafted and crosslinked with PDAPipCl. A transparent and flexible HEM prepared in this way, with an IEC of 2.34 meq. g^{-1} and water uptake of 128%, reached an OH^- conductivity of 101 mS cm^{-1} at 80 °C. It should be noted that this procedure was developed only to demonstrate that the *N*-spirocyclic polyelectrolytes can be employed for membrane use and the materials were not optimized.

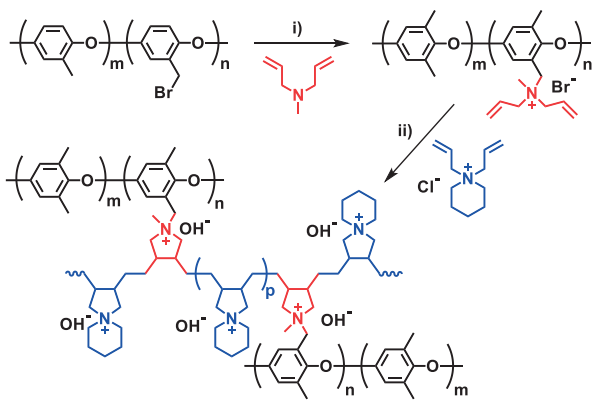

Scheme 8. Preparation of PPO-based HEMs grafted and crosslinked with an *N*-spirocyclic QA polyelectrolyte. key: i) NMP, 40 °C, ii) AIBN, NMP/methanol, 75 °C and ion-exchange in NaOH

To sum up Paper I, one of the main findings in this work was that, as long as an *N*-spirocyclic QA cation is suitably designed, polyelectrolytes with very high thermal and alkaline stability can be easily prepared in high yield from commercially available and cheap chemicals. We also showed, on a conceptual level, a method to prepare HEMs from these water-soluble *N*-spirocyclic polyelectrolytes. Continued work included attempts to graft benzyl-brominated PPO with PDAPipCl using atom transfer radical polymerization (ATRP), but these efforts were unsuccessful.

Later work on HEMs based on DADMAC-type polymers included two especially interesting publications, in which membrane-forming polymers were prepared from telechelic precursor polymers. Balsara et al. reported on HEMs based on poly(DADMAC-styrene) diblock copolymers prepared in subsequent reversible addition-fragmentation chain-transfer (RAFT) polymerizations.[167] Knauss et al. prepared multiblock polysulfone copolymers in nucleophilic aromatic substitution reactions using fluorophenyl sulfone terminated PDAPipCl.[168] The materials presented in the latter publication were promising enough to be protected by a patent application.[169] However, the polysulfone block in these materials must most probably be replaced with a more alkali-stable alternative in order to obtain HEMs with long-term *in-situ* stability.

4.2 Poly(arylene piperidinium) HEMs (Paper II-IV)

After the work with diallylammonium monomers was concluded, the exploration of other methods to prepare HEMs functionalized with piperidine-based cations was resumed and the polyhydroxyalkylation reaction was brought into our attention. On paper, this superacid mediated polycondensation, where highly rigid and ether-free polymers carrying pendant piperidine units are produced, looked perfect. The polymerization reaction was both quick and straightforward, and our desired structure could be obtained using cheap and available chemicals. Besides, several factors such as cation structure, IEC and water uptake could easily be tuned and the effect on the *ex-situ* membrane properties assessed. The HEMs presented in Papers II, III and IV were all prepared from different poly(arylene piperidinium)s (PAPipQ)s synthesized in polyhydroxyalkylation reactions of biphenyl or *p*-terphenyl with piperidone. Paper II-III will be presented together, while Paper IV is discussed on its own due to its different focus.

4.2.1 The effect of an alkyl chain (Paper II)

Polymer design and synthesis

In Paper II a series of HEMs based on poly(*p*-terphenyl *N*,*N*-methyl*alkyl* piperidinium)s were synthesized and characterized. As shown in **Scheme 9**, the only variation in the molecular structure between these polymers was the length of the *N*-alkyl chain. All polymers and HEMs were prepared from the same precursor polymer, a poly(*p*-terphenyl piperidine) (PTPip), which was synthesized by polymerization of *p*-terphenyl and *N*-methyl piperidone in a TFSA mediated polyhydroxyalkylation reaction. In this reaction, the ketone monomer was added in excess (1.3 eq.) in order to increase the rate of polymerization. The obtained PTPip could not be analyzed

using gel-permeation chromatography (GPC) due to issues with both solubility and sample adsorption to the column. Instead, an indication of the molar mass was obtained by measuring the intrinsic viscosity of the polymer in DMSO (0.1 M LiBr) at 30 °C. The intrinsic viscosity [η] for PTPip was 0.39 dl g^{-1} and corresponded to a medium molar mass.

Optimization of the polymerization reaction conditions in order to achieve high molar mass was difficult without the assistance of the GPC. However, to increase the molar mass, and decrease the rate of the side reaction (described in detail in the experimental methods section), all polymerizations were conducted at 0 °C and stopped before the reaction viscosity started to decrease.

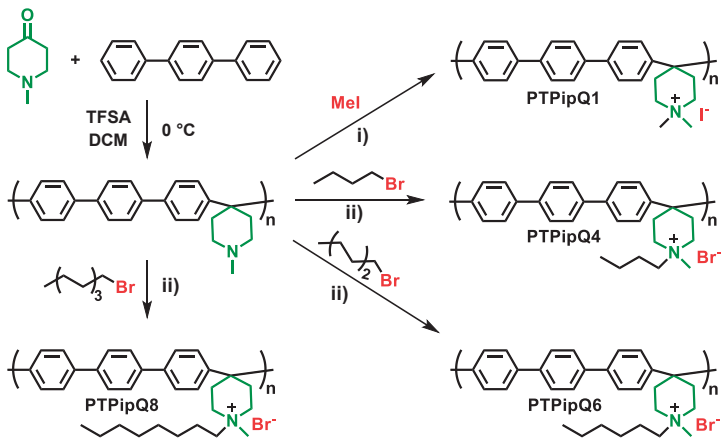

Scheme 9. Preparation and molecular structure of the different PTPipQ*x* HEMs presented in Paper II. *key: i) DMSO, room temperature, ii) DMSO/NMP, 80 °C*

Next, PTPip was quaternized with methyl, butyl, hexyl and octyl halides, respectively, to prepare four cationic polymers with alkyl chains of varying length (**Scheme 9**). These polymers were designated PTPipQ*x*, where *x* denotes the alkyl chain length in number of carbon atoms. After purification, transparent and robust HEMs were prepared by solvent casting and used for subsequent characterization.

Characterization

By introducing alkyl chains of varying length both the IEC and the phase separation characteristics of the HEMs could be directly influenced, which in turn affected the water uptake and ion conductivity. These properties, together with the decomposition temperature ($T_{d,95}$) of the prepared HEMs can be found in **Table 2**. Unsurprisingly, the water uptake followed the IEC, and decreased with increasing alkyl chain length. At 80 °C, the water uptake reached 404, 290, 171 and 79 wt% for PTPipQ1, -Q4, -

Q6 and -Q8, respectively. The length of the alkyl chains also had a clear effect on the scattering profile of the HEMs, which was studied using SAXS. While PTPipQ1 only showed a diffuse scattering peak at 4.5 nm, there was a clear trend for the samples with longer alkyl chain. Both the intensity of the ionomer peak and the separation distance increased with the alkyl chain length, and PTPipQ4, -Q6 and -Q8 displayed clear peaks at d ≈ 1.2, 1.4 and 1.5 nm, respectively (**Table 2**). Hence, the attachment of longer alkyl chains clearly promoted a phase separated morphology, as compared to PTPipQ1.

Table 2. Properties of the PTPipQx polymers and the corresponding HEMs.

HEM	IEC [a] /meq. g^{-1}		$T_{d,95}$[b] /°C	WU[c] /wt%	σ[c] /mS cm^{-1}	d[d] /nm
	theoretical[a]	titrated				
PTPipQ1	2.38 (2.80)	2.42	264	404	89	4.5
PTPipQ4	2.16 (2.50)	2.21	250	290	84	1.2
PTPipQ6	2.04 (2.34)	2.08	241	171	111	1.4
PTPipQ8	1.93 (2.19)	1.98	232	79	61	1.5

[a] Calculated from the molar mass of the repeating unit in Br^- form (OH^- form). [b] Evaluated from TGA data obtained under N_2 at 10 °C min^{-1}. [c] Measured under immersed conditions in OH^- form at 80 °C. [d] In the dry Br^- form measured by SAXS.

The measured OH^- conductivity of the HEMs followed neither IEC nor water uptake. Instead, PTPipQ6, with IEC and water uptake lower than PTPipQ1 and -Q4, exhibited the highest OH^- ion conductivity as it reached 111 mS cm^{-1} at 80 °C. This observation can be explained by the extreme water uptake observed for both PTPipQ1 and -Q4, which most likely led to dilution of the charge carriers and, hence, a decreased conductivity.[44] PTPipQ8, with the most developed phase separated morphology, probably still had a too low water uptake to form a well-percolating water phase and therefore exhibited the lowest ion conductivity. All in all, in regard to water uptake and conductivity, PTPipQ6, with an *N*,*N*-methylhexylpiperidinium cation, was the best performing HEM. To be clear, this observation was most probably related to the IEC and water uptake of the HEMs, and was not a direct effect of the structure of the cation.

The thermal stability of the HEMs was also clearly affected by the alkyl chain length and the $T_{d,95}$ values decreased with increasing chain length and ranged between 232 and 264 °C (**Table 2**).

Alkaline stability

The final, and perhaps most interesting, property left to discuss is the *ex-situ* alkaline stability of the HEMs. Similar to in Paper I, this was assessed by studying ^{1}H NMR

spectra of the samples taken after different storage times in 2 M aq. NaOH at 90 °C. The resulting spectra for PTPipQ1 and -Q8 before and after storage are shown in **Figure 20**. Emerging signals at 5.0, 5.4 and 6.6 ppm (*1-3,* **Figure 20c-d**), which originate from vinylic protons (–C*H*=CH_2) formed in Hofmann elimination reactions, were observed for all samples. Because these signals were also present in the spectra of PTPipQ1, they cannot stem from products formed in elimination reactions of the alkyl chain itself. Instead the signals must originate from elimination reactions in the piperidinium ring leading to ring-opening as shown in **Figure 20c-d**. This was the major degradation pathway of all four samples, and the rate of degradation was strongly correlated to the length of the alkyl chain and followed the same trend as the thermal stability.

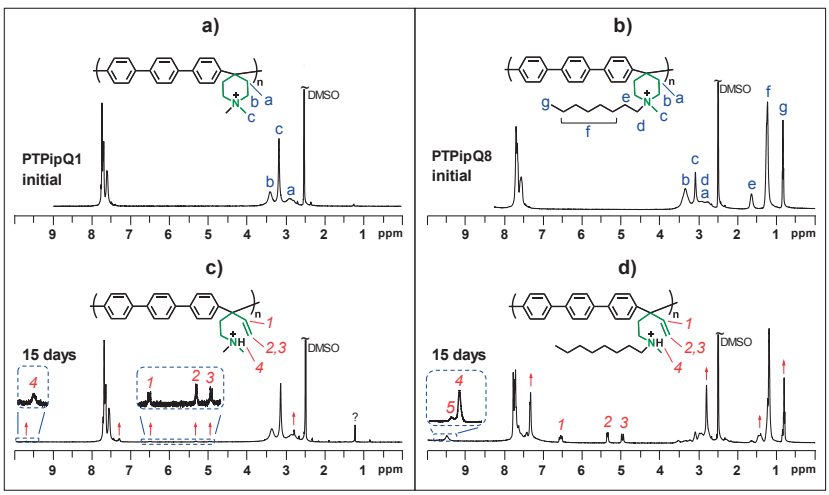

Figure 20. ^{1}H NMR spectra of PTPipQ1 and -Q8 before (a-b) and after (c-d) storage in 2M aq. NaOH at 90 °C. Characteristic signals emerging due to Hofmann elimination have been assigned (*1-4*). Other emerging signals are denoted with red arrows. The signal denoted *5* implies the existence of an additional degradation reaction.

Addition of TFA to the NMR solutions caused protonation of all tertiary amines formed in degradation reactions and two distinct signals (*4* and *5*, **Figure 20d**) appeared at ~9.5 ppm for all samples but PTPipQ1, where only one signal appeared (*4*, **Figure 20c**). After integration and comparison of all the emerging signals, it was concluded that the larger upfield signal (*4*) corresponded to the tertiary amine formed in the Hofmann ring-opening elimination, while the other smaller signal (*5*) must correspond to another type of degradation mechanism, most likely, Hofmann elimination or nucleophilic substitution leading to the loss of the alkyl chain and formation of an *N*-methylpiperidine moiety. The formation of *N*-methyl piperidine was further supported by the position of *5*, which overlapped fully with the

corresponding signal of the non-quaternized, but protonated, precursor polymer PTPip.

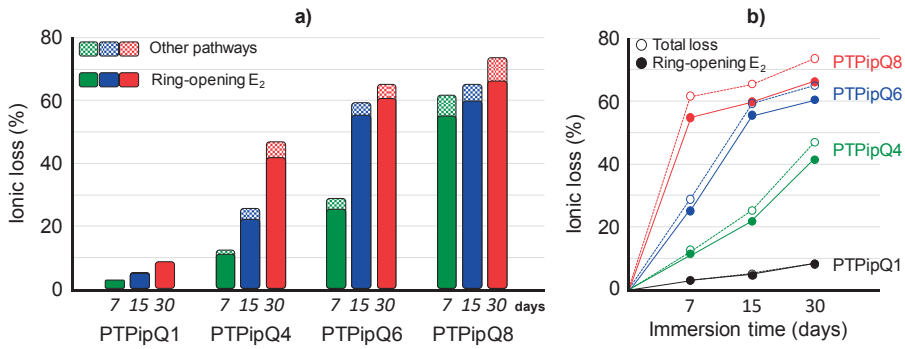

Figure 21. a) Total ionic loss for the PTPipQx-series after storage in 2 M aq. NaOH at 90 °C for 7 (green), 15 (blue) and 30 days (red). The solid and patterned part of the bars represents the degree of degradation *via* Hofmann elimination (E_2) causing ring-opening and other, unassigned, pathways, respectively. b) Ionic loss (same data as in a) as a function of immersion time.

The amount of degradation or degree of ionic loss was determined by integration of relevant NMR signals and comparison with all signals from aromatic protons (7-8 ppm). Since only one degradation mechanism was confirmed, the ionic loss was divided into two categories, shown in **Figure 21a-b**. Total ionic loss (open circles, **Figure 21b**); calculated by the combined integrals of *4* and *5,* and ionic loss *via* Hofmann ring-opening elimination (solid bars and circles, **Figure 21a-b**); calculated by the average integral of *1*, *2* and *3*. The discrepancy between total ionic loss and the degree of Hofmann ring-opening elimination is denoted other pathways (patterned bars, **Figure 21a**). As can be seen, the introduction of longer alkyl chains had a clear negative effect on the alkaline stability of the HEMs. Both types of degradation seemed to increase with the alkyl chain length. PTPipQ1 exhibited a total ionic loss of a mere ≈5% during 15 days in 2 M aq. NaOH at 90 °C, while PTPipQ8 lost more than 60% of the original QA cations after only 7 days under the same conditions. As can be seen in **Figure 21b**, the initial degradation rate (slope) was approximately constant, but at 50-60% cationic loss, a plateau was reached. This observation might be related to a decrease in water uptake and that the OH^- ions no longer had access to some of the remaining cations. PTPipQ1 and PTPipQ8 were also studied after 15 days at 60 °C in 2 M aq. NaOH. At this temperature, no degradation was observed for PTPipQ1, while PTPipQ8 lost approximately 3% of the cations.

From the alkaline stability study in Paper II it was concluded that the *N*,*N*-dimethylpiperidinium (DMP) cation was the most alkali-stable of the tested cations. Even though it degraded in 2 M aq. NaOH at 90 °C, being stable at 60 °C is still quite

difficult to achieve and a noteworthy result. However, we were not fully satisfied, so in order to increase the stability further we revisited the study conducted by Marino and Kreuer.[11] In their study, the DMP cation only placed second (**Figure 9**). Its half-life in 6 M aq. NaOH at 160 °C was surpassed by the bis-6-membered *N*-spirocyclic ASU cation.[11] Thus, in order to further explore and, hopefully, improve the stability of PAPipQ-type HEMs, continued work was focused on the incorporation of *N*-spirocyclic cations and the alkaline stability of the resulting HEMs.

4.2.2 Introducing *N*-spirocyclic cations (Paper III)

Polymer design and synthesis

Although the process from monomer to *N*-spirocyclic functionalized HEM included procedures similar to those used in Paper II, there were some differences, as shown in **Scheme 10**. First, a secondary 4-piperidone was used in the polymerization reaction to enable a subsequent quaternization reaction where spirocyclic cations could be formed. Second, control over the IEC to limit the water uptake was introduced by the addition of non-ionic comonomers to the polyhydroxyalkylation reaction. 1,1,1-trifluoroacetone (TFAc) or 2,2,2-trifluoroacetophenone (TFAp) was polymerized together with 4-piperidone and biphenyl to prepare two precursor

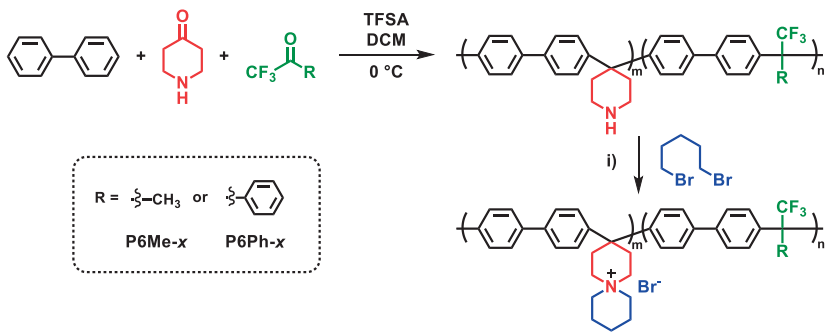

Scheme 10. Preparation of P6Me-*x* and P6Ph-*x* *via* TFSA mediated copolymerization and subsequent cyclo-quaternization. *key: i) DIPEA, NMP/DMSO, 80 °C*

polymers (**Scheme 10)**. Finally, a dihalide, dibromopentane, was used in the ring-closing cyclo-quaternization reaction. The obtained quaternized polymers were designated P6Me-*x* and P6Ph-*x*, where *x* is the IEC in OH^- form as calculated from Mohr titration data. In the published article (Paper III), several other HEMs were also prepared and studied, but to keep this summary brief and to the point only two polymers are included.

Alkaline stability

To enable a direct comparison with the alkaline stability results for the PTPipQ*x*-series in Paper II, the HEMs carrying *N*-spirocyclic cations were studied using the same procedure. A representative ^{1}H NMR spectrum obtained after storage in 2 M aq. NaOH at 90 °C after 30 days is shown in **Figure 22**. Changes in the spectrum have been marked with red arrows. Significant emerging signals have been magnified (red dashed boxes) and correspond to degradation *via* Hofmann ring-opening elimination. In contrast to the results for the PTPipQ*x*-series, two different sets of vinylic signals have appeared, indicating that degradation occurred in both rings. Further analysis revealed that the backbone ring (red-colored, *a-c*) was more susceptible to ring-opening than the pendant ring (blue-colored, *d-f*).

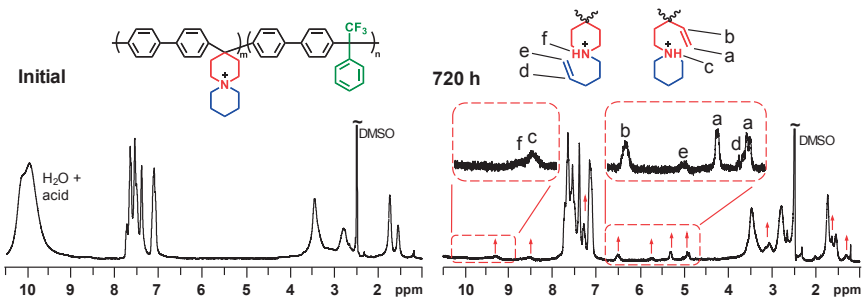

Figure 22. ^{1}H NMR spectra of P6Ph-1.8 before (left) and after (right) storage in 2 M aq. NaOH at 90 °C. The magnified signals have been assigned to protons of Hofmann degradation products.

Interestingly, our results showed that the *N*-spirocyclic ASU cation performed worse than the monocyclic DMP one, when attached to a rigid polymer. The total ionic loss exceeded 20% during 30 days for P6Ph-1.8, as compared to a loss of around 8% for PTPipQ1 during the same time. This is the opposite relationship of that observed by Marino and Kreuer in their study on small molecules.[11] However, in that study neither the DMP nor the ASU cation degraded *via* Hofmann ring-opening elimination. Since this was the primary degradation mechanism observed by us, it must have been enabled by other factors in our molecular design. The culprit was most likely the substituents in the 4-position of the piperidinium ring and/or the placement of the piperidinium ring within a stiff polymer backbone.

4.2.3 Hofmann ring-opening elimination of *N*-alicyclic QA cations

In order to get a better understanding of what enabled the Hofmann ring-opening elimination observed for the PAPipQs, a model compound was synthesized and studied. The compound, 4,4-diaryl-*N*,*N*-dimethylpiperidinium iodide, was prepared in order to investigate the effect of bulky substituents in the 4-position of a

piperidinium ring. After exposure to 2 M aq. NaOH at 120 °C for 14 days, no sign of degradation was observed by NMR analysis. This strongly indicated that bulky substituents in the 4-position of the piperidinium could not, alone, be responsible for the Hofmann elimination observed for the polymer samples studied at 90 °C.

Instead, we believe that the alkaline stability of the *N*-alicyclic cations was severely reduced due to restrictions of the conformational freedom of the ring-system caused mostly by the rigid backbone. These restrictions limited the possibility for ring relaxation and forced the ring to stay in high energy conformations, which in turn led to a lower activation energy for ring-opening reactions and enabled otherwise unfavorable reaction mechanisms.

A similar observation had also been made in a study by our group on two different *N*-spirocyclic ionenes with identical cations.[108] In that study, the polymer with a flexible spacer unit between cations was much more stable than the other consisting of more rigid structure. The rigid structure also exhibited degradation *via* Hofmann ring-opening elimination, while the sample with the more flexible structure did not.[108]

How the alkyl chain could have the large effect on the alkaline stability that was observed in Paper II is perhaps not as straightforward to explain. An increased degradation rate arising from the introduction of an alkyl chain with vulnerable β-hydrogens is normally explained by degradation reactions involving the alkyl chain itself.[124] For example, in a citation of our work, Yan et al. ascribed the increased degradation rate for PTPipQ4, -Q6 and –Q8 exclusively to elimination reactions leading to loss of the alkyl chain.[76] However, the data from Paper II strongly suggested that degradation occurred predominantly in the ring for all samples, leaving the alkyl chain attached to the polymer. We believe that the increased degradation rate was due to further limitations of the ring relaxation process originating from the placement of the alkyl chain (an additional bulky substituent) on the ring.

4.2.4 Introducing control over IEC and water uptake (Paper IV)

While the polymers presented in Papers I - III were all prepared with focus on their alkaline stability, the emphasis in Paper IV was to introduce control over the IEC and the water uptake of PAPipQ-type polymers in order to prepare HEMs with more balanced properties. The results of Paper II clearly showed that the high ionic content of PTPipQ1 caused excessive water uptake, which compromised both mechanical properties and OH^-conductivity. To overcome this, three different strategies were developed and implemented: partial quaternization, copolymerization (similar to Paper III) and crosslinking, as shown in **Figure 23**. The prepared HEMs were then characterized with focus on IEC, water uptake and OH^- conductivity.

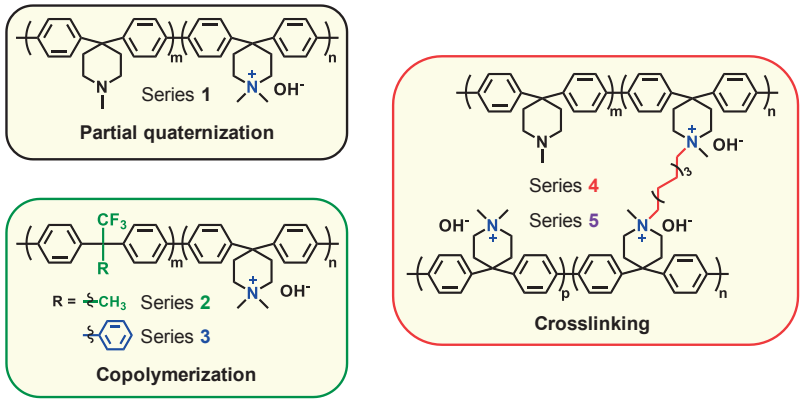

Figure 23. The molecular structures obtained using different approaches to prepare HEMs with balanced IEC, water uptake and OH^- conductivity. The samples have been separated into Series 1-5 depending on molecular structure.

The polymer synthesis followed mainly previously developed (and described) methods and proceeded *via* polyhydroxyalkylation followed by quaternization. All reaction products were verified using ^1H NMR spectroscopy and the degree of quaternization was analyzed by Mohr titrations. As can be seen in **Figure 23**, all polymers were based on a biphenyl backbone with piperidinium type cations. Several HEMs of varying IEC were prepared using each approach and some of their properties can be found in **Table 3**. In order to be able to easily address HEMs of different design, they were divided into 5 series depending on how they were made and their molecular content (**Figure 23**). For example, two series (Series 2 and 3) both consisted of samples prepared by the copolymerization approach, but with different comonomers. Each series have also been assigned its own color and designation, as shown in **Table 3**. For example, PBPipQ*XxY*, where *Xx* is the percentage of ionic repeating units. *Y* denotes the comonomer used, TFAc (Ac) or TFAp (Ap). For the partially quaternized samples *Y* = %. The crosslinked samples will be discussed later.

For all samples both water uptake and OH^- conductivity increased with increasing IEC. Generally, samples in Series 1 showed a higher water uptake at a given IEC than those in Series 2 and 3 (**Table 3**). An observation that might be related to the different hydrophilicity of the non-ionic repeating units. The polar non-ionic repeating units in Series 1 (tertiary amines) probably contributed to an overall more hydrophilic polymer compared to the more hydrophobic non-ionic repeating units in Series 2 and 3, which were made up of TFAc and TFAp residues, respectively. At least one sample in each series reached >100 mS cm^{-1} at 80 °C. However, in this kind of study it is more interesting to study water uptake as a function of IEC and conductivity as a

Table 3. Selected properties of the HEMs in Series 1 – 3.

HEM	IEC [a] /meq. g^{-1}	WU[b] /wt%	λ[c]	σ[b] /mS cm^{-1}	Series
PBPipQ35%	1.34	58	24	27	1
PBPipQ42%	1.59	117	39	65	
PBPipQ52%	1.95	200	55	104	
PBPipQ64%	2.37	278	64	168	
PBPipQ44Ac	1.7	65	21	50	2
PBPipQ51Ac	1.92	85	25	88	
PBPipQ60Ac	2.25	143	35	143	
PBPipQ42Ap	1.39	34	13	49	3
PBPipQ56Ap	1.91	92	27	67	
PBPipQ66Ap	2.26	141	35	118	

[a] In OH^- form, calculated from Mohr titration data. [b] Measured under immersed conditions in OH^- form at 80 °C. [c] λ = [H2O]/[QA^+] at 80 °C.

function of water content (λ), as shown in **Figure 24a and b**, respectively. As can be seen, the samples in Series 2 and 3 performed comparably, with very similar water uptake at a given IEC and comparable conductivity at similar water content. The introduction of hydrophobic comonomers allowed for the preparation of HEMs with moderate water uptake and high conductivity. In contrast, as can be seen for samples in Series 1 (**Figure 24b**), the presence of polar, but non-ionic, tertiary amines only seemed to boost the water uptake, without markedly contributing to the OH^- conductivity. In general, the HEMs in Series 1 exhibited a much larger water uptake at a given IEC and were only able to reach >100 mS cm^{-1} at very high λ values.

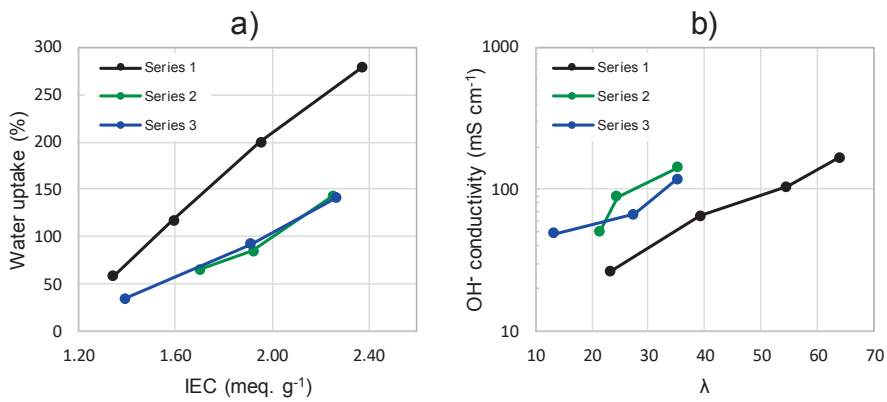

Figure 24. a) Water uptake of the HEMs, in Series 1 – 3, in OH^- form at 80 °C as function of IEC and b) OH^- conductivity under fully hydrated conditions at 80 °C as a function of λ.

Crosslinking

Even though the IEC of the HEMs in Series 1 had been limited by partial quaternization, the samples still exhibited large water uptakes at high ionic content. With the aim of decreasing water uptake and improving the mechanical properties, crosslinked HEMs were prepared from the same precursor polymer that was used for Series 1. This non-quaternized poly(biphenyl piperidine) was first crosslinked by solvent casting in the presence of a predetermined stoichiometric shortage of 1,8-dibromooctane. During the casting, part of the *N*-methylpiperidine moieties were quaternized and linked together. Next, the residual piperidine units were partially quaternized to obtain HEMs with IECs ranging from 1.7 to 2.3 meq. g^{-1}. In total, five crosslinked HEMs, divided into two sets of samples, Series 4 and 5 with ~18 and ~35% of the amines being part of crosslinks (degree of crosslinking), respectively, were prepared. Their performance in comparison with samples in Series 1 can be seen in **Figure 25a-b**, where water uptake *vs.* IEC (a) and OH^- conductivity *vs.* λ (b) is shown.

As can be seen in **Figure 25a**, water uptake decreased significantly with the degree of crosslinking. For example, at a given IEC, the samples in Series 5 (35% degree of crosslinking) exhibited approximately half the water uptake of the samples in Series 1. **Figure 25b** shows that the conductivity at a given λ was highest for samples in Series 5 and lowest for Series 1. Hence, the crosslinking was successful and each water molecule in the crosslinked materials contributed more to conductivity, as compared to the water in HEMs in Series 1. At 80 °C, the best performing crosslinked HEM reached a conductivity of 102 mS cm^{-1} at an IEC of 2.26 meq. g^{-1} and 116% water uptake.

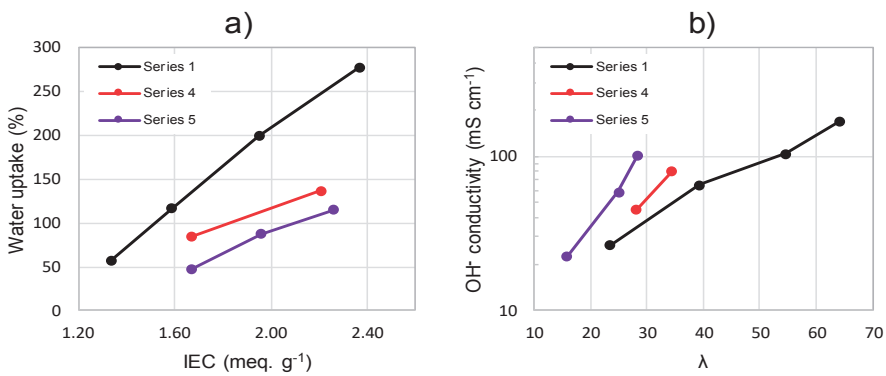

Figure 25. Comparison between the crosslinked HEMs in Series 4 and 5 and the HEMs in Series 1. a) Water uptake in the OH^- form at 80 °C as function of IEC and b) OH^- conductivity under fully hydrated conditions at 80 °C as a function of λ.

Alkaline stability

The alkaline stability of the prepared HEMs was analyzed by immersion in 2 M aq. NaOH at 90 °C for 20 days and the results are shown in **Table 4**. Four samples, one each from Series 1-3 and one from Series 5, with similar IEC (1.90-1.95 meq. g^{-1}) were tested. The ionic loss for the insoluble crosslinked sample was analyzed by Mohr titration and the other's using NMR spectroscopy. The discrepancy between the ionic loss from Hofmann elimination and total elimination, observed for samples in Series 1-3, originate from an unassigned emerging NMR signal at 8.5 ppm (Spectra in Fig. 6, Paper III). This signal was only visible after addition of TFA and was too large to be overlooked. Since this signal did not overlap with the tertiary *N*-methylpiperidine moiety in the precursor polymer, it could not be the results of methyl substitution reactions. Instead, the signal might have arisen due to tertiary amines formed in ring-opening substitution reactions and the total ionic loss was calculated with the assumption that this signal corresponded to 1 proton per lost charge.

After 20 days, the ionic loss due to Hofmann ring-opening elimination reaction amounted to 6, 12 and 13% for samples in Series 1, 2 and 3, respectively (**Table 4**). Since these samples all carried the same type of cation (DMP), the variance in the observed stability was ascribed to the quite large difference in water uptake (**Table 3**) between the samples. At a higher water uptake ring relaxation might occur to a greater extent and the OH^- can be expected to be more hydrated and less aggressive. The results in Paper IV can be compared to PTPipQ1 (Paper II), which lost approximately 6% of the cations after 20 days in 2 M aq. NaOH at 90 °C.

Table 4. Ionic loss after 20 days storage in 2 M aq. NaOH at 90 °C calculated from ^{1}H NMR spectra (Series 1-3) and titration data (Series 5)

HEM	Hofmann /%	Total /%	Series
PBPipQ52%	6	11	1
PBPipQ51Ac	12	14	2
PBPipQ56Ap	13	15	3
Crosslinked	n.d.	51[a]	5

[a] Calculated from Mohr titration data.

According to titration data, the crosslinked sample lost more than half of its cations after 20 days (**Table 4**). Thus, the introduction of octyl crosslinkers dramatically increased the rate of degradation. This was expected and the mechanism was assumed to be the same as postulated for the PTPipQs with *N*-alkyl extender chains, discussed previously.

Summary PAPipQ

Overall, the results of Papers II-IV show that PAPipQ polymers with very interesting structures can be efficiently prepared from commercially available monomers. Subsequent HEMs had a high alkaline stability and performance as long as the DMP cation was employed. Introduction of *N*-alkyl extender chains severely destabilized the cyclic cation and increased the rate of ionic loss, especially *via* Hofmann ring-opening elimination. The overall performance of the HEMs suffered from high water uptake and water swelling. Even though a comprehensive study where different methods to solve the problem (Paper IV) produced significantly improved HEMs, their performance was still hampered by this. These issues were probably a consequence of not being able to synthesize polymers of high enough molar mass due to the difficulties with the irreversible side reaction occurring during the polymerizations. Over the course of the work, membranes were easily formed from the prepared polymers and an increase of the molar mass was not expected to give major improvements. Thus, efforts to further optimize the polymerization was deprioritized due to the high pace and competitiveness of the field. In hindsight, that assessment was perhaps not valid, which became clear after Yan et al. published a paper on polymers and HEMs structurally similar to those presented in Paper II.[76] Yan's polymers exhibited an intrinsic viscosity as high as 4.71 dl g^{-1}, which is 12 times higher than for PTPipQ1 (0.39 dl g^{-1}). One of their materials, with an IEC of 2.37 meq. g^{-1}, was able to reach very high conductivity (>150 mS cm^{-1}) at moderate water uptake <60% at 80 °C.[76] Hence, their results led us to believe that most of the water uptake related issues (dilution effects etc.) we had with our HEMs might have been resolved or avoided if we had been able to prepare polymers of higher molar mass.

Continued work

Since the project on poly(arylene piperidinium) polymers was initiated, the polyhydroxyalkylation reaction has been diligently used in our group to prepare various aromatic polymers[124, 170, 171] and even more that has not yet been published.

By investing in a better cooling system (better than ice bath) and using a mechanical stirrer for the polyhydroxyalkylation reactions, we have managed to achieve AEMs with lower water uptake at high ionic content. The result is promising, and more improvements can be expected with further optimization.

4.3 *N*-alicyclic QA functional polystyrene (Paper V)

The exploration of new polymers carrying *N*-alicyclic QA cations was continued after the work with the poly(arylene piperidinium) polymers presented in Papers II-IV. With basis in the observations made in previous stability studies, a new *N*-alicyclic QA cation functional polymer was developed. The idea was focused on retaining the inherently high alkaline stability of the *N*-alicyclic QA cation by maintaining a high conformational freedom of the ring and keeping the constraints on the ring relaxation to a minimum.[11] One way of achieving this, is by using flexible components, *e.g.* attaching the cation to a flexible backbone. A widely used flexible polymer backbone is polystyrene (PS).[40, 95-97, 172] PS based HEMs are typically prepared by quaternization of poly(vinylbenzyl chloride), but the resulting structure is not alkali-stable, due to the benzylic placement of the cation (**Figure 26a**).[11] To improve the stability, the cation can be separated from the backbone and the benzylic position by the use of a tether.[58, 114] It is important that the tether itself does not introduce any vulnerable functionalities, such as β-hydrogens available for elimination as shown in **Figure 26b**.[124] Instead, a rationally designed tether is connected in the 4-position of the piperidinium ring **(Figure 26c)**. All β-hydrogens in such a structure are located within the ring and should be stabilized against Hofmann elimination. Additionally, this type of tether allows for subsequent cyclo-quaternization and for the preparation *N*-spirocyclic cations. A suitable synthetic procedure, with basis in literature[153], was developed in order to achieve a structure similar to the one shown in **Figure 26c**.

Thus, presented in the fifth and final Paper of this thesis, was a facile two-step synthetic strategy through which polystyrene (PS) was functionalized with mono-and spiro-cyclic piperidine-based cations. As can be seen in **Scheme 11**, the obtained structure contained no additional heteroatoms (*e.g.* ether bonds) and all β-hydrogens were located within the alicyclic rings. HEMs prepared from these polymers

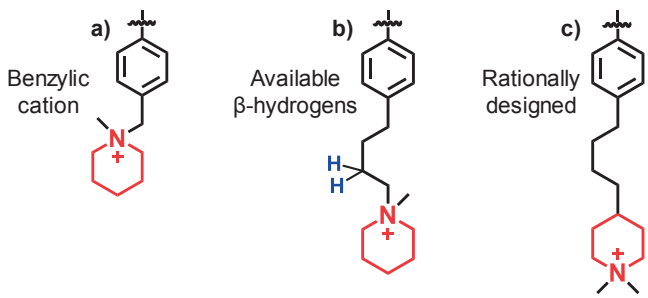

Figure 26. Charged units on a polymer chain with cations attached *via* tethers of different design.

exhibited high water uptake and high conductivity. However, due to the low T_g and bad membrane-forming ability of PS, the mechanical properties of the HEMs were poor. In order to overcome this, blend membranes of PS carrying *N*,*N*-dimethylpiperidinium cations and polybenzimidazole (PBI-O) were prepared.

Polymer functionalization

Initially, PS (M_n = 170 kg mol^{-1}, PDI = 2.06) was functionalized in superacid mediated Friedel-Crafts hydroxyalkylation reactions using 2-(piperidine-4-yl)propane-2-ol) (Pip*t*OH), shown in **Scheme 11**. In these reactions a consistent amount of approximately 50% of the Pip*t*OH added to the vessel reacted with the PS and it was possible to reach a degree of functionalization (DF) of just below 30%. Aiming for higher DF produced insoluble materials. In total, three precursor polymers with DF of 19, 22 and 27% were prepared.

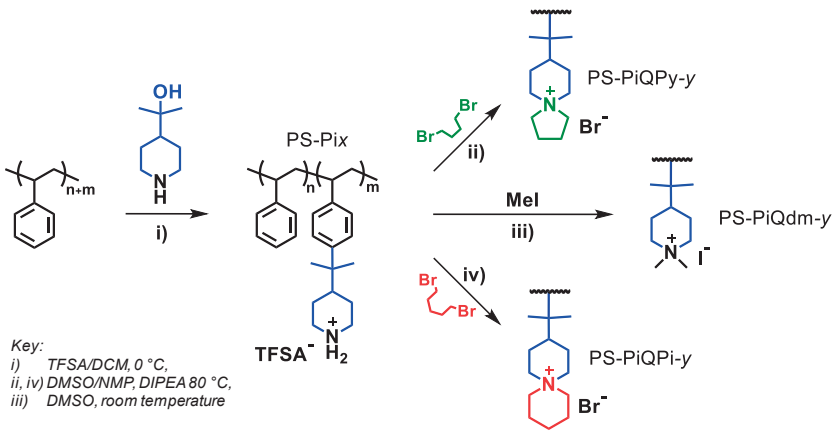

Scheme 11. Two-step synthesis of *N*-alicyclic QA functional PS *via* hydroxyalkylation and (cyclo)-quaternization.

Using DSC, the glass transition temperature (T_g) of the prepared precursors was obtained. As expected, the flexibility of the PS chain was decreased by the addition of a bulky functional group and the T_g of all the precursor polymers increased to ~125°C from 105 °C, obtained for the neat PS.

In subsequent reactions (**Scheme 11**), the precursor polymers were quaternized using 1,4-dibromobutane or 1,5-dibromopentane, respectively, to prepare polymers carrying *N*-spirocyclic cations denoted PS-PiQPy-*y* and PS-PiQPi-*y*, respectively. In addition, iodomethane was used to prepare three polymers carrying DMP cations (PS-PiQdm-*y*) of different IEC. Here, *y* is the IEC in the OH^- form, which was calculated from Mohr titration data and ranged between 1.3 and 1.7 meq. g^{-1}. HEMs were then

prepared by casting at 70 °C from DMSO solutions in Petri dishes. Some selected properties of the obtained HEMs are shown in **Table 5**.

Table 5. Properties of the HEMs based on *N*-alicyclic functional PS

Sample	DF [a] /%	$IEC_{Titr.}$ [b] /meq. g^{-1}	$T_{d,95}$ [c] /°C	WU_{80} [d] /wt%	σ_{80} [d] /mS cm^{-1}
PS-PiQdm-1.4	19	1.37	305	85	64
PS-PiQdm-1.5	22	1.50	271	120	106
PS-PiQdm-1.7	27	1.73	245	268	79
PS-PiQPy-1.3	19	1.34	341	70	52
PS-PiQPi-1.3	19	1.32	331	53	37

[a] Degree of functionalization (DF) of the precursor polymers calculated from ^{1}H NMR data. [b] In OH^- form calculated from Mohr titration of samples in Br^- form. [d] Measured on fully hydrated AEMs at 80 °C in both the Br^- and the OH^- form, respectively.

Characterization

Studying the thermal decomposition of the HEMs by TGA showed that PS-PiQPy-1.3 and PS-PiQPi-1.3, with *N*-spirocyclic cations, showed a higher thermal stability than the DMP functional ones, which agreed with our previous studies. PS-PiQPy-1.3 displayed the highest $T_{d,95}$, while the $T_{d,95}$ of the PS-PiQdm series decreased with increasing ionic content (**Table 5)**.

The water uptake of the HEMs in the OH^- form followed the IEC and reached 53 – 268%. PS-PiQPy-1.3 and PS-PiQPi-1.3, with *N*-spirocyclic cations, took up less water than PS-PiQdm-1.4 prepared from the same precursor polymer. The lower water uptake was also coupled to an observed lower OH^- conductivity. These observations can probably be explained by a combination of the lower IEC of PS-PiQPy-1.3 and PS-PiQPi-1.3 and the more hydrophobic character of the *N*-spirocyclic cations in comparison to DMP. The highest OH^- conductivity was measured for PS-PiQdm-1.5 (106 mS cm^{-1}), which was substantially higher than observed for the sample with the highest IEC, PS-PiQdm-1.7. Hence, the conductivity of PS-PiQdm-1.7 likely suffered from dilution effect due to the high water uptake. In general, the PS HEMs were mechanically weak and easily torn apart despite their high molar mass. On top of this, the HEMs became opaque when exposed to water (they were fully transparent after casting). This phenomenon was connected to the water uptake, as it was more pronounced for samples with higher IEC and in the OH^- form.

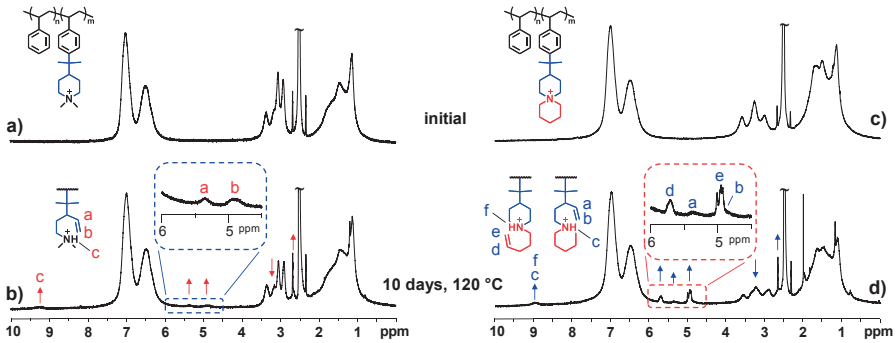

Figure 27. ^{1}H NMR spectra of a-b) PS-PiQdm-1.4 and c-d) PS-PiQPi-1.3 before and after storage in 2 M aq. NaOH at 120 °C for 10 days. The spectra were obtained with DMSO-d_6 solutions with added TFA.

The alkaline stability of PS-PiQdm-1.4, PS-PiQPy-1.3 and PS-PiQPi-1.3 was assessed by studying structural changes by NMR spectroscopy after storage in 2 M aq. NaOH at 90 and 120 °C. Since PS-PiQPy-1.3 became insoluble after the tests it was not analyzed further. After 30 days at 90 °C, only minor signs of degradation could be observed for both samples indicating a high alkaline stability of both cations. However, after 10 days at 120 °C clear signs of degradation were observed, as can be seen in **Figure 27b and d**. Vinylic signals from ring-opening Hofmann elimination were observed at 4.9 and 5.4 ppm in both spectra (*a* and *b*). An additional set of vinylic signals were observed for PS-PiQPi-1.3 (*d* and *e*), which indicated that degradation occurred in both rings. By comparing the position of the emerged signals with those observed for PS-PiQdm-1.4, it was concluded that the ring furthest from the backbone degraded fastest (red-colored). In total PS-PiQdm-1.4 and PS-PiQPi-1.3 degraded <1 and <5% at 90 °C, respectively, and approximately 13 and 25% at 120 °C. The *N*-spirocyclic cation only degraded *via* ring-opening Hofmann-elimination, while the discrepancy between intensity of the vinylic signals and the signals originating from protonated tertiary amines at 9.2 ppm indicated that another degradation mechanism was active for the mono-cyclic cation. The most likely candidates include methyl substitution or ring-opening substitution. As compared to the results of the alkaline stability studies for PTPipQ1, the DMP cation in PS-PiQdm-1.4 showed a significantly enhanced resistance towards ring-opening Hofmann elimination. Thus, the introduction of a flexible backbone and tether to increase the alkaline stability of the DMP cation was successful.

Further analysis of the NMR spectra on tested polymer samples, revealed that all signals from protons on the functional group seemed to decreased with increased storage time in the alkaline solution. This was also observed in a spectrum where no other signs degradation could be distinguished, as can be seen in **Figure 28a**. Hence,

the mechanism was assumed to be unrelated to the cation degradation discussed above. After some consideration, we came up with two plausible hypotheses for this observation. The most obvious one involves cleavage of the benzylic C-C bond, leading to the loss of the entire functional group (**Figure 28b**). The other involves loss of highly functionalized polymer strands (higher than average) by dissolution and leeching during the alkaline testing (**Figure 28c**).

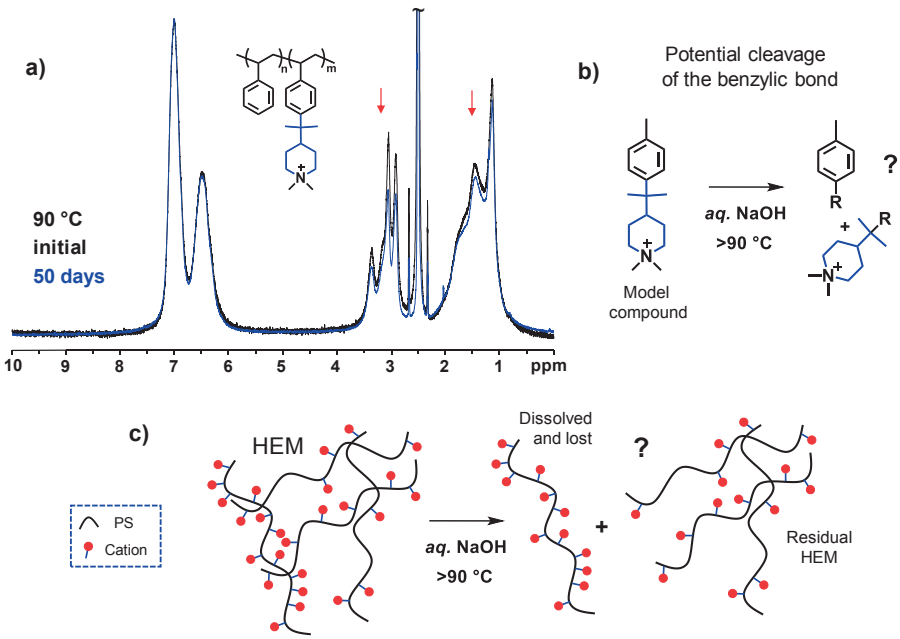

Figure 28. a) ^{1}H NMR spectra of PS-PiQdm-1.4 before (black) and after (blue) storage in 2 M aq. NaOH at 90 °C for 50 days. Illustration of the two hypotheses: b) potential cleavage of the benzylic C-C bond, here shown in a model compound, leading to loss of the functional group and c) possible dissolution and loss of a highly functionalized PS strand.

Model compound and leeching hypothesis

To assess if the benzylic C-C bond was cleaved during storage at elevated temperature in alkaline media, a model compound, 2-(dimethyl piperidinium-4-yl)propan-2-tolyl (**Figure 28b**), was prepared and tested for 10 days at 120 °C in both 2 M and 5 M aq. NaOH. Storage in the former caused no observable changes at all, while treatment in 5 M aq. NaOH only gave rise to small signals indicating ring-opening *via* Hofmann elimination. Hence, no indications of cleavage of the benzylic bond was observed. This was further strengthened by other studies on HEMs and polymers carrying similar tethers, where no such cleavage was reported.[85, 86]

The second hypothesis was tested by analyzing if any cationic PS could be found in the alkaline solution after storage at 120 °C in 0.1 M aq. NaOH during 10 days. After the treatment the HEM sample was washed, dried and weighed, while the alkaline solution was carefully evaporated. The solid contents were then quantitatively dissolved in DMSO-d_6 and analyzed by NMR. The resulting spectra clearly showed the presence of cationic PS, which had a significantly higher average DF (73%) as compared to the HEM (27%) and was, hence, more water soluble. Approximately 3 wt% of the HEM sample was lost through the leeching process, corresponding to around 8% of the total number of cations.

To explain the presence of these highly functionalized PS strands, the nature of the functionalization reaction in which they were prepared must be considered. This reaction progressed as a two-phase system (suspension) due to the low solubility of PS in the DCM/TFSA mixture. During the reaction, the suspension was homogenized by gradual dissolution of functionalized PS. Thus, the functionalized PS became more soluble and had better access to the electrophile (Pip*t*OH) than the less soluble non-functionalized PS. In such a reaction, where functionalization promotes more functionalization, the product will most likely be inhomogeneously functionalized. In this case, the distribution of the degree of functionalization was very broad and the most functionalized polymer strands were soluble enough in water to leech out of the HEM at elevated temperature.

The opacity observed for the hydrated PS HEMs might also be related to the to the inhomogeneity of the material. It is possible that hydration of the HEMs caused hydrophobic PS (low DF) to precipitate and scatter visible light, hence making the HEM opaque. On top of this, the mechanical properties would also suffer if part of the PS precipitated.

Blending

Blending was employed as an approach to prepare HEMs based on PS functionalized with *N*-alicyclic piperidine based cations with improved mechanical properties. In this special case, blending will most probably also prevent the dissolution and loss of highly functionalized PS, which was observed for the PS HEMs. The blend membranes were prepared by co-casting PS-PiQdm-1.7 and a commercially available polybenzimidazole (PBI-O). By immersing the obtained blend HEMs in alkaline solution, piperidinium-imidazole complexes were formed. These complexes function as ionic crosslinks that limit swelling both physically and by decreasing the effective IEC of the HEM. The crosslinks are stable as long as the membranes are kept under alkaline conditions.

In total, three blend membranes containing 2, 5 and 10 wt% PBI-O (denoted PS-PBIO-*x*%) in addition to PS-PiQdm-1.7 were prepared. Handling the blend membranes after storage in 1 M aq. NaOH during 48 h clearly indicated that the mechanical properties of the blend membranes had improved, in comparison to PS-PiQdm-1.7 in the OH^- form. The issue with membrane opacity was much less pronounced for the blend HEMs as well.

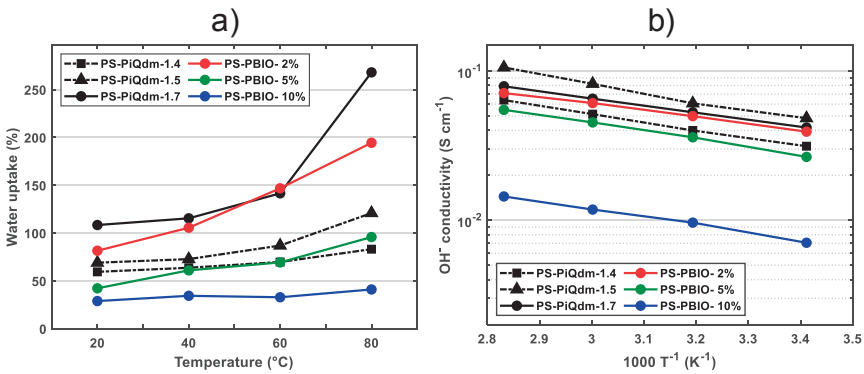

Figure 29. a) Water uptake and b) ion conductivity in the OH^- form of the blend HEMs (colored) and the PS-PiQdm series (black).

In **Figure 29a-b**, the water uptake and OH^- conductivity of the blend HEMs as well as the pure PS HEMs are shown as a function of temperature. The colored lines correspond to the blend HEMs and the black ones to PS-PiQdm samples. At a given temperature, the water uptake and OH^- conductivity of the blend HEMs increased, as expected, with increasing theoretical IEC (decreasing amount of PBI-O). In comparison with PS-PiQdm-1.7, the best performing blend HEM (PS-PBIO-2%) showed a 28% reduction in water uptake accompanied by a 10% drop in conductivity. Though, based exclusively on the data shown in **Figure 29**, PS-PBIO-2% was outperformed by PS-PiQdm-1.5, which exhibited a higher OH^- conductivity at a lower water uptake. However, this data does not take the improved mechanical properties into account. With more optimization of the blending procedure, *e.g.* using a PS with higher DF, further improvement of the blend HEMs can most likely be accomplished.

Summary

In Paper V, a two-step synthetic procedure to prepare PS functionalized with *N*-alicyclic cations was presented. Piperidine moieties, attached in 4-position, were first introduced *via* a superacid mediated Friedel Crafts alkylation reaction. In subsequent quaternizations both mono- and *N*-spirocyclic cations were formed in Menshutkin

reactions with alkyl halides. An HEM based on PS functionalized with DMP cations showed the highest alkaline stability, with no observed cation degradation after 50 days at 90 °C. The high stability against ring-opening degradation reactions was ascribed to the flexible backbone as well as the presence of an isopropylidene spacer in-between the PS backbone and the cationic rings. These features significantly mitigated Hofmann degradation in comparison with PAPipQs carrying the same cation. Despite a moderate IEC, the PS HEMs could reach high OH^- conductivity (*e.g.* 106 mS cm^{-1} at 80 °C, 1.5 meq. g^{-1}). However due to the inherently poor membrane forming ability of PS, the mechanical properties of the prepared PS HEMs was inadequate. By blending with PBI-O, it was possible to prepare blend HEMs with improved mechanical properties accompanied by only a small reduction in conductivity. In the bigger picture, the results of this study showed that by replacing benchmark BTMA cations with *N*-alicyclic QA cations, the alkaline stability of cationic PS can be significantly enhanced and the feasibility of employing these types of polymers in HEMFCs improved.

5 Conclusion and outlook

5.1 Conclusion

In this thesis a variety of cationic polymers have been designed, synthesized and characterized in order to gain valuable knowledge in the ongoing development of high-performance HEMs for fuel cell use. The main focus has been to prepare alkali-stable *N*-alicyclic QA cation functional polymers from commercially available materials in straightforward synthetic procedures. By rational polymer design, this was successfully achieved in as little as two steps by modification of procedures found in literature. In total, three distinctly different strategies to prepare *N*-alicyclic QA cation functional polymers were developed and a total number of 36 HEMs was prepared and characterized. The studied polymers included water soluble poly(*N*,*N*-diallylazacycloalkane)s (Paper I), poly(arylene piperidinium) (PAPipQ) type polymers (Paper II-IV) and *N*-alicyclic QA cation functionalized PS (Paper V).

Even though one of the polyelectrolytes (PDAPipCl) in Paper I exhibited a very high alkaline stability, the water solubility of these polymers and the synthetic limitations of the diallylammonium monomers made it difficult to employ this type of polyelectrolyte as the cationic moieties for HEMs. In contrast, HEMs with good mechanical properties were easily formed from the PAPipQs (Paper II-IV) prepared in superacid mediated polycondensations. These polymers combined a very rigid and stable arylene backbone with alkali-stable *N*-alicyclic QA cations. However, due to conformational constraints of the cationic rings generated by the stiff polymer backbone, ring-opening degradation reactions were facilitated and the inherently high alkaline stability of the cation was to some extent reduced. In regard to alkaline stability and ability to form membranes, the functionalized PS (Paper V) ranked in the middle. HEMs were easily prepared, but due to the low T_g and high flexibility of the PS backbone, they were mechanically poor and prone to excessive water swelling. However, the extra flexibility did lessen the constraints on the *N*-alicyclic QA cation, compared to the PAPipQs, and the alkaline stability was improved. In the studies on PAPipQs and PS HEMs, the polymers carrying *N*,*N*-dimethylpiperidinium cations (DMP) were more stable than corresponding polymer with *N*-spirocyclic cations or *N*,*N*-methylalkylpiperidinium cations. Hence, attachment of additional large moieties on the ring seemed to increase the degradation rate.

The work presented herein has, in particular, highlighted how the alkaline stability of different cationic polymers is affected by the structure and placement of different *N*-alicyclic cations. It was demonstrated that, in order to preserve the cation's inherently

high alkaline stability, shown in studies on small molecules, it is imperative that ring-relaxation is enabled in the final polymer structure.

5.2 Outlook

The continued work with polymers carrying *N*-alicyclic QA cations is already ongoing in the group. Much of the work is still focused on the development of poly(arylene alkylene) type polymers prepared in superacid mediated polyhydroxyalkylation reactions. In general, we are trying to improve the cation stability by separating the cation from the backbone *via* a flexible tether using different chemistry. Here the main goal is to design a procedure and prepare HEMs with good mechanical properties carrying *N*-alicyclic QA cations with high conformational freedom and alkaline stability.

With more time, it would have been interesting to try and develop a synthetic procedure where the cationic repeating unit in the functionalized PS (Paper V) could be incorporated into a hydrophobic membrane-forming polymer. An obstacle to overcome in such a project would be to find either a pre- or post-polymerization functionalization procedure that is compatible with superacid chemistry.

None of the HEMs presented in this thesis has yet been tested in an actual fuel cell. In previous collaborations with electrochemists, we have received complaints on membrane inhomogeneity and thickness variation. This has become especially important since membrane thickness appeared to be one of the main parameters determining the fuel cell output in our latest collaboration.[173] In order to be able to deliver better HEMs for testing we have invested in a mini tape casting coater and method development is ongoing. In the future we will deliver PTPipQ type polymer membranes to KTH for fuel cell testing and evaluation.

6 References

1. IEA, Paris, *World Energy Outlook*, **2016**. https://www.iea.org/reports/world-energy-outlook-2016
2. Lewis, N. S.; Nocera, D. G. *Proc. Natl. Acad. Sci. U. S. A.* **2006,** 103, (43), 15729-15735.
3. Gielen, D.; Boshell, F.; Saygin, D.; Bazilian, M. D.; Wagner, N.; Gorini, R. *Energy Strategy Rev.* **2019,** 24, 38-50.
4. Chu, S.; Majumdar, A. *Nature* **2012,** 488, 294.
5. Aricò, A. S.; Bruce, P.; Scrosati, B.; Tarascon, J.-M.; van Schalkwijk, W. *Nat. Mater.* **2005,** 4, (5), 366-377.
6. Goodenough, J. B.; Park, K.-S. *J. Am. Chem. Soc.* **2013,** 135, (4), 1167-1176.
7. Carmo, M.; Fritz, D. L.; Mergel, J.; Stolten, D. *Int. J. Hydrogen Energy* **2013,** 38, (12), 4901-4934.
8. Carrasco, J. M.; Franquelo, L. G.; Bialasiewicz, J. T.; Galvan, E.; PortilloGuisado, R. C.; Prats, M. A. M.; Leon, J. I.; Moreno-Alfonso, N. *IEEE Trans. Ind. Electron.* **2006,** 53, (4), 1002-1016.
9. Kirubakaran, A.; Jain, S.; Nema, R. K. *Renew. Sustain. Energy Rev* **2009,** 13, (9), 2430-2440.
10. Wang, Y.; Chen, K. S.; Mishler, J.; Cho, S. C.; Adroher, X. C. *Appl. Energy* **2011,** 88, (4), 981-1007.
11. Marino, M. G.; Kreuer, K.-D. *ChemSusChem* **2015,** 8, (3), 513-523.
12. Ran, J.; Wu, L.; He, Y.; Yang, Z.; Wang, Y.; Jiang, C.; Ge, L.; Bakangura, E.; Xu, T. *J. Membr. Sci.* **2017,** 522, 267-291.
13. Wang, W.; Luo, Q.; Li, B.; Wei, X.; Li, L.; Yang, Z. *Adv. Funct. Mater.* **2013,** 23, (8), 970-986.
14. Logan, B. E.; Elimelech, M. *Nature* **2012,** 488, 313.
15. Leng, Y.; Chen, G.; Mendoza, A. J.; Tighe, T. B.; Hickner, M. A.; Wang, C.-Y. *J. Am. Chem. Soc.* **2012,** 134, (22), 9054-9057.
16. Zhang, H.; Shen, P. K. *Chem. Rev.* **2012,** 112, (5), 2780-2832.

17. Kreuer, K.-D., *Fuel Cells*. Springer: New York, 2013.

18. Wee, J.-H. *Renew. Sustain. Energy Rev* **2007,** 11, (8), 1720-1738.

19. Chung, H. T.; Cullen, D. A.; Higgins, D.; Sneed, B. T.; Holby, E. F.; More, K. L.; Zelenay, P. *Science* **2017,** 357, (6350), 479-484.

20. Hong, S.; Hou, M.; Zhang, H.; Jiang, Y.; Shao, Z.; Yi, B. *Electrochim. Acta* **2017,** 245, 403-409.

21. Duclos, L.; Lupsea, M.; Mandil, G.; Svecova, L.; Thivel, P.-X.; Laforest, V. *J. Clean. Prod.* **2017,** 142, (Part 4), 2618-2628.

22. Franklin, G. W.; James, C. D. Fluorocarbon vinyl ether polymers, U.S. Patent 3282875A, 1966.

23. Kreuer, K.-D. *Chem. Mater.* **2014,** 26, (1), 361-380.

24. Kreuer, K.-D. *J. Membr. Sci.* **2001,** 185, (1), 29-39.

25. Kraytsberg, A.; Ein-Eli, Y. *Energy Fuels* **2014,** 28, (12), 7303-7330.

26. Kusoglu, A.; Weber, A. Z. *Chem. Rev.* **2017,** 117, (3), 987-1104.

27. Merle, G.; Wessling, M.; Nijmeijer, K. *J. Membr. Sci.* **2011,** 377, (1–2), 1-35.

28. Varcoe, J. R.; Slade, R. C. T. *Fuel Cells* **2005,** 5, (2), 187-200.

29. Varcoe, J. R.; Atanassov, P.; Dekel, D. R.; Herring, A. M.; Hickner, M. A.; Kohl, P. A.; Kucernak, A. R.; Mustain, W. E.; Nijmeijer, K.; Scott, K.; Xu, T.; Zhuang, L. *Energy Environ. Sci.* **2014,** 7, (10), 3135.

30. Dekel, D. R. *J. Power Sources* **2018,** 375, 158-169.

31. Varcoe, J. R.; Slade, R. C. T.; Lam How Yee, E. *Chem. Commun.* **2006**, (13), 1428-1429.

32. Lu, S.; Pan, J.; Huang, A.; Zhuang, L.; Lu, J. *Proc. Natl. Acad. Sci. U. S. A.* **2008,** 105, (52), 20611.

33. Couture, G.; Alaaeddine, A.; Boschet, F.; Ameduri, B. *Prog. Polym. Sci.* **2011,** 36, (11), 1521-1557.

34. Gottesfeld, S.; Dekel, D. R.; Page, M.; Bae, C.; Yan, Y.; Zelenay, P.; Kim, Y. S. *J. Power Sources* **2018,** 375, 170-184.

35. Arges, C. G.; Zhang, L. *ACS Appl. Energy Mater.* **2018,** 1, (7), 2991-3012.

36. Hickner, M. A. *Electrochem Soc. Interface* **2017,** 26, (1), 69-73.

37. Jannasch, P.; Weiber, E. A. *Macromol. Chem. Phys.* **2016,** 217, (10), 1108-1118.

38. Maurya, S.; Fujimoto, C. H.; Hibbs, M. R.; Narvaez Villarrubia, C.; Kim, Y. S. *Chem. Mater.* **2018,** 30, (7), 2188-2192.

39. Dang, H.-S.; Jannasch, P. *ACS Appl. Energy Mater.* **2018,** 1, (5), 2222-2231.

40. Wang, L.; Bellini, M.; Miller, H. A.; Varcoe, J. R. *J. Mater. Chem. A* **2018,** 6, (31), 15404-15412.

41. Zhu, L.; Yu, X.; Peng, X.; Zimudzi, T. J.; Saikia, N.; Kwasny, M. T.; Song, S.; Kushner, D. I.; Fu, Z.; Tew, G. N.; Mustain, W. E.; Yandrasits, M. A.; Hickner, M. A. *Macromolecules* **2019,** 52, (11), 4030-4041.

42. Chen, W.; Mandal, M.; Huang, G.; Wu, X.; He, G.; Kohl, P. A. *ACS Appl. Energy Mater.* **2019,** 2, (4), 2458-2468.

43. Varcoe, J. R.; Kizewski, J. P.; Halepoto, S. D.; Slade, R. C. T.; Zhao, F., Anion-Exchange Membranes. In *Encyclopedia of Electrochemical Power Sources*, Garche, J.; Dyer, C. K., Eds. Elsevier: 2009.

44. Marino, M. G.; Melchior, J. P.; Wohlfarth, A.; Kreuer, K. D. *J. Membr. Sci.* **2014,** 464, 61-71.

45. Hickner, M. A.; Herring, A. M.; Coughlin, E. B. *J. Polym. Sci., Part B: Polym. Phys.* **2013,** 51, (24), 1727-1735.

46. Hugar, K. M.; Kostalik, H. A.; Coates, G. W. *J. Am. Chem. Soc.* **2015,** 137, (27), 8730-8737.

47. Mohanty, A. D.; Bae, C. *J. Mater. Chem. A* **2014,** 2, (41), 17314-17320.

48. Dekel, D. R.; Willdorf, S.; Ash, U.; Amar, M.; Pusara, S.; Dhara, S.; Srebnik, S.; Diesendruck, C. E. *J. Power Sources* **2018,** 375, 351-360.

49. Marx, D.; Chandra, A.; Tuckerman, M. E. *Chem. Rev.* **2010,** 110, (4), 2174-2216.

50. Tuckerman, M. E.; Marx, D.; Parrinello, M. *Nature* **2002,** 417, (6892), 925-929.

51. de Grotthuss, C. *Ann. Chim.* **1806,** 58, 54-74.

52. Marx, D. *ChemPhysChem* **2006,** 7, (9), 1848-1870.

53. Chen, M.; Zheng, L.; Santra, B.; Ko, H.-Y.; DiStasio Jr, R. A.; Klein, M. L.; Car, R.; Wu, X. *Nat. Chem.* **2018,** 10, (4), 413-419.

54. Peckham, T. J.; Holdcroft, S. *Adv. Mater.* **2010,** 22, (42), 4667-4690.

55. Kreuer, K.-D. *Solid State Ion.* **2013,** 252, 93-101.

56. Li, N.; Yan, T.; Li, Z.; Thurn-Albrecht, T.; Binder, W. H. *Energy Environ. Sci.* **2012,** 5, (7), 7888-7892.

57. Dang, H.-S.; Jannasch, P. *Macromolecules* **2015,** 48, (16), 5742-5751.

58. Dang, H.-S.; Weiber, E. A.; Jannasch, P. *J. Mater. Chem. A* **2015,** 3, (10), 5280-5284.

59. Dang, H.-S.; Jannasch, P. *J. Mater. Chem. A* **2016,** 4, (43), 17138-17153.

60. Wohlfarth, A.; Smiatek, J.; Kreuer, K.-D.; Takamuku, S.; Jannasch, P.; Maier, J. *Macromolecules* **2015,** 48, (4), 1134-1143.

61. Zhou, J.; Unlu, M.; Vega, J. A.; Kohl, P. A. *J. Power Sources* **2009,** 190, (2), 285-292.

62. Zhang, F.; Zhang, H.; Qu, C. *J. Mater. Chem.* **2011,** 21, (34), 12744-12752.

63. Arges, C. G.; Ramani, V. *Proc. Natl. Acad. Sci. U.S.A.* **2013,** 110, (7), 2490-2495.

64. Weiber, E. A.; Jannasch, P. *ChemSusChem* **2014,** 7, (9), 2621-2630.

65. Chen, D.; Hickner, M. A. *ACS Applied Materials & Interfaces* **2012,** 4, (11), 5775-5781.

66. Weiber, E. A.; Meis, D.; Jannasch, P. *Polymer Chemistry* **2015,** 6, (11), 1986-1996.

67. Amel, A.; Zhu, L.; Hickner, M.; Ein-Eli, Y. *J. Electrochem. Soc.* **2014,** 161, (5), F615-F621.

68. Mohanty, A. D.; Tignor, S. E.; Krause, J. A.; Choe, Y.-K.; Bae, C. *Macromolecules* **2016,** 49, (9), 3361-3372.

69. Dang, H.-S.; Jannasch, P. *J. Mater. Chem. A* **2016,** 4, (30), 11924.

70. Dang, H.-S.; Jannasch, P. *Macromolecules* **2015,** 48, (16), 5742.

71. Dang, H.-S.; Weiber, E. A.; Jannasch, P. *J. Mater. Chem. A* **2015,** 3, (10), 5280.

72. Akiyama, R.; Yokota, N.; Miyatake, K. *Macromolecules* **2019,** 52, (5), 2131-2138.

73. Lee, W.-H.; Mohanty, A. D.; Bae, C. *ACS Macro Lett.* **2015,** 4, (4), 453-457.

74. Lee, W.-H.; Park, E. J.; Han, J.; Shin, D. W.; Kim, Y. S.; Bae, C. *ACS Macro Lett.* **2017,** 6, (5), 566-570.

75. Lee, W.-H.; Kim, Y. S.; Bae, C. *ACS Macro Lett.* **2015,** 4, (8), 814-818.

76. Wang, J.; Zhao, Y.; Setzler, B. P.; Rojas-Carbonell, S.; Ben Yehuda, C.; Amel, A.; Page, M.; Wang, L.; Hu, K.; Shi, L.; Gottesfeld, S.; Xu, B.; Yan, Y. *Nat. Energy* **2019**.

77. Olsson, J. S.; Pham, T. H.; Jannasch, P. *J. Membr. Sci.* **2019,** 578, 183-195.

78. Pham, T. H.; Olsson, J. S.; Jannasch, P. *J. Mater. Chem. A* **2019**.

79. Pham, T. H.; Olsson, J. S.; Jannasch, P. *J. Mater. Chem. A* **2018,** 6, (34), 16537-16547.

80. Olsson, J. S.; Pham, T. H.; Jannasch, P. *Adv. Funct. Mater.* **2017,** 28, 1702758.

81. Peng, H.; Li, Q.; Hu, M.; Xiao, L.; Lu, J.; Zhuang, L. *J. Power Sources* **2018,** 390, 165-167.

82. Ren, R.; Zhang, S.; Miller, H. A.; Vizza, F.; Varcoe, J. R.; He, Q. *ACS Appl. Energy Mater.* **2019,** 2, (7), 4576-4581.

83. Hibbs, M. R. *J. Polym. Sci., Part B: Polym. Phys.* **2013,** 51, (24), 1736-1742.

84. Hibbs, M. R.; Fujimoto, C. H.; Cornelius, C. J. *Macromolecules* **2009,** 42, (21), 8316-8321.

85. Jeon, J. Y.; Park, S.; Han, J.; Maurya, S.; Mohanty, A. D.; Tian, D.; Saikia, N.; Hickner, M. A.; Ryu, C. Y.; Tuckerman, M. E.; Paddison, S. J.; Kim, Y. S.; Bae, C. *Macromolecules* **2019,** 52, (5), 2139-2147.

86. Jeon, J. Y.; Mohanty, A. D.; Tian, D.; Bae, C. *ECS Trans.* **2017**, 80, (8), 967-970

87. Hao, J.; Gao, X.; Jiang, Y.; Zhang, H.; Luo, J.; Shao, Z.; Yi, B. *J. Membr. Sci.* **2018,** 551, 66-75.

88. Mohanty, A. D.; Ryu, C. Y.; Kim, Y. S.; Bae, C. *Macromolecules* **2015,** 48, (19), 7085-7095.

89. Sun, L.; Guo, J.; Zhou, J.; Xu, Q.; Chu, D.; Chen, R. *J. Power Sources* **2012,** 202, 70-77.

90. Su, X.; Gao, L.; Hu, L.; Qaisrani, N. A.; Yan, X.; Zhang, W.; Jiang, X.; Ruan, X.; He, G. *J. Membr. Sci.* **2019,** 581, 283-292.

91. Clark, T. J.; Robertson, N. J.; Kostalik Iv, H. A.; Lobkovsky, E. B.; Mutolo, P. F.; Abruña, H. D.; Coates, G. W. *J. Am. Chem. Soc.* **2009,** 131, (36), 12888-12889.

92. Wang, C.; Mo, B.; He, Z.; Shao, Q.; Pan, D.; Wujick, E.; Guo, J.; Xie, X.; Xie, X.; Guo, Z. *J. Membr. Sci.* **2018,** 556, 118-125.

93. Mandal, M.; Huang, G.; Kohl, P. A. *ACS Appl. Energy Mater.* **2019,** 2, (4), 2447-2457.

94. Wang, X.; Sheng, W.; Shen, Y.; Liu, L.; Dai, S.; Li, N. *J. Membr. Sci.* **2019,** 587, 117135.

95. Varcoe, J. R.; Slade, R. C. T.; Lam How Yee, E.; Poynton, S. D.; Driscoll, D. J.; Apperley, D. C. *Chem. Mater.* **2007,** 19, (10), 2686-2693.

96. Ponce-González, J.; Whelligan, D. K.; Wang, L.; Bance-Soualhi, R.; Wang, Y.; Peng, Y.; Peng, H.; Apperley, D. C.; Sarode, H. N.; Pandey, T. P.; Divekar, A. G.; Seifert, S.; Herring, A. M.; Zhuang, L.; Varcoe, J. R. *Energy Environ. Sci.* **2016,** 9, (12), 3724-3735.

97. Gonçalves Biancolli, A. L.; Herranz, D.; Wang, L.; Stehlíková, G.; Bance-Soualhi, R.; Ponce-González, J.; Ocón, P.; Ticianelli, E. A.; Whelligan, D. K.; Varcoe, J. R.; Santiago, E. I. *J. Mater. Chem. A* **2018,** 6, (47), 24330-24341.

98. Wang, L.; Peng, X.; Mustain, W. E.; Varcoe, J. R. *Energy Environ. Sci.* **2019,** 12, (5), 1575-1579.

99. Lin, X.; Liang, X.; Poynton, S. D.; Varcoe, J. R.; Ong, A. L.; Ran, J.; Li, Y.; Li, Q.; Xu, T. *J. Membr. Sci.* **2013,** 443, 193-200.

100. Sherazi, T. A.; Yong Sohn, J.; Moo Lee, Y.; Guiver, M. D. *J. Membr. Sci.* **2013,** 441, 148-157.

101. You, W.; Noonan, K. J. T.; Coates, G. W. *Prog. Polym. Sci.* **2020,** 100, 101177.

102. Hugar, K. M.; Kostalik, H. A.; Coates, G. W. *J. Am. Chem. Soc.* **2015,** 137, (27), 8730.

103. Fan, J.; Wright, A. G.; Britton, B.; Weissbach, T.; Skalski, T. J. G.; Ward, J.; Peckham, T. J.; Holdcroft, S. *ACS Macro Lett.* **2017**, 1089-1093.

104. Wright, A. G.; Weissbach, T.; Holdcroft, S. *Angew. Chem. Int. Ed.* **2016,** 55, (15), 4818-4821.

105. Thomas, O. D.; Soo, K. J. W. Y.; Peckham, T. J.; Kulkarni, M. P.; Holdcroft, S. *J. Am. Chem. Soc.* **2012,** 134, (26), 10753-10756.

106. Hugar, K. M.; You, W.; Coates, G. W. *ACS Energy Lett.* **2019,** 4, (7), 1681-1686.

107. Parrondo, J.; Wang, Z.; Jung, M.-S. J.; Ramani, V. *PCCP* **2016,** 18, (29), 19705-19712.

108. Pham, T. H.; Olsson, J. S.; Jannasch, P. *J. Am. Chem. Soc.* **2017,** 139, (8), 2888-2891.

109. Olsson, J. S.; Pham, T. H.; Jannasch, P. *Macromolecules* **2017,** 50, (7), 2784-2793.

110. Faraj, M.; Elia, E.; Boccia, M.; Filpi, A.; Pucci, A.; Ciardelli, F. *J. Polym. Sci., Part A: Polym. Chem.* **2011,** 49, (15), 3437-3447.

111. Zha, Y.; Disabb-Miller, M. L.; Johnson, Z. D.; Hickner, M. A.; Tew, G. N. *J. Am. Chem. Soc.* **2012,** 134, (10), 4493-4496.

112. Gu, S.; Cai, R.; Luo, T.; Jensen, K.; Contreras, C.; Yan, Y. *ChemSusChem* **2010,** 3, (5), 555-558.

113. Sun, Z.; Lin, B.; Yan, F. *ChemSusChem* **2018,** 11, (1), 58-70.

114. Tomoi, M.; Yamaguchi, K.; Ando, R.; Kantake, Y.; Aosaki, Y.; Kubota, H. *J. Appl. Polym. Sci.* **1997,** 64, (6), 1161-1167.

115. Clayden, J.; Greeves, N.; Warren, S. G., *Organic chemistry*. Oxford University Press: Oxford; New York, 2012.

116. Hamlin, T. A.; Swart, M.; Bickelhaupt, F. M. *ChemPhysChem* **2018,** 19, (11), 1315-1330.

117. Marino, M. G. Anion exchange membranes for fuel cells and flow batteries : transport and stability of model systems. Ph.D. Thesis, University of Stuttgart, 2015.

118. Cope, A. C.; Mehta, A. S. *J. Am. Chem. Soc.* **1963,** 85, (13), 1949-1952.

119. Bauer, B.; Strathmann, H.; Effenberger, F. *Desalination* **1990,** 79, (2), 125-144.

120. Jones, F. N.; Hauser, C. R. *J. Org. Chem.* **1962,** 27, (5), 1542-1547.

121. Pine, S. H., The Base-Promoted Rearrangements of Quaternary Ammonium Salts. In *Organic Reactions*, John Wiley & Sons, Inc., 2004.

122. Stevens, T. S.; Creighton, E. M.; Gordon, A. B.; MacNicol, M *J. Chem. Soc* **1928**, 3193-3197.

123. Long, H.; Pivovar, B. *J. Phys. Chem. C* **2014,** 118, (19), 9880-9888.

124. Allushi, A.; Pham, T. H.; Olsson, J. S.; Jannasch, P. *J. Mater. Chem. A* **2019,** 7, (47), 27164-27174.

125. Nuñez, S. A.; Capparelli, C.; Hickner, M. A. *Chem. Mater.* **2016,** 28, (8), 2589-2598.

126. Ponce-González, J.; Varcoe, J. R.; Whelligan, D. K. *ACS Appl. Energy Mater.* **2018,** 1, (5), 1883-1887.

127. Butler, G. B.; Bunch, R. L. *J. Am. Chem. Soc.* **1949,** 71, (9), 3120-3122.

128. Butler, G. B.; Ingley, F. L. *J. Am. Chem. Soc.* **1951,** 73, (3), 895-896.

129. Butler, G. B.; Goette, R. L. *J. Am. Chem. Soc.* **1952,** 74, (8), 1939-1941.

130. Butler, G. B.; Bunch, R. L.; Ingley, F. L. *J. Am. Chem. Soc.* **1952,** 74, (10), 2543-2547.

131. Butler, G. B.; Johnson, R. A. *J. Am. Chem. Soc.* **1954,** 76, (3), 713-714.

132. Butler, G. B.; Goette, R. L. *J. Am. Chem. Soc.* **1954,** 76, (9), 2418-2421.

133. Butler, G. B.; Angelo, R. J. *J. Am. Chem. Soc.* **1956,** 78, (18), 4797-4800.

134. Butler, G. B.; Angelo, R. J. *J. Am. Chem. Soc.* **1957,** 79, (12), 3128-3131.

135. Butler, G., *Cyclopolymerization and Cyclocopolymerization*. Taylor & Francis: 1992. pp 5-6.

136. Wandrey, C.; Hernández-Barajas, J.; Hunkeler, D., Diallyldimethylammonium Chloride and its Polymers. In *Radical Polymerisation Polyelectrolytes*, Capek, I.; Hernfández-Barajas, J.; Hunkeler, D.; Reddinger, J. L.; Reynolds, J. R.; Wandrey, C., Eds. Springer Berlin Heidelberg: Berlin, Heidelberg, 1999; pp 123-183.

137. Butler, G. B. Water Soluble Quaternary Ammonum Polymers, U.S. Patent 3288770A 1966.

138. Jaeger, W.; Bohrisch, J.; Laschewsky, A. *Prog. Polym. Sci.* **2010,** 35, (5), 511-577.

139. Baeyer, A. *Ber. Dtsch. Chem. Ges* **1872,** 5, (1), 280-282.

140. Olah, G. A. *Angew. Chem. Int. Ed.* **1993,** 32, (6), 767-788.

141. Olah, G. A.; Prakash, G. K. S.; Sommer, J.; Molnar, A., *Superacid Chemistry*. Wiley: 2009.

142. Olvera, L. I.; Guzmán-Gutiérrez, M. T.; Zolotukhin, M. G.; Fomine, S.; Cárdenas, J.; Ruiz-Trevino, F. A.; Villers, D.; Ezquerra, T. A.; Prokhorov, E. *Macromolecules* **2013,** 46, (18), 7245-7256.

143. Cruz, A. R.; Hernandez, M. C. G.; Guzmán-Gutiérrez, M. T.; Zolotukhin, M. G.; Fomine, S.; Morales, S. L.; Kricheldorf, H.; Wilks, E. S.; Cárdenas, J.; Salmón, M. *Macromolecules* **2012,** 45, (17), 6774-6780.

144. Diaz, A. M.; Zolotukhin, M. G.; Fomine, S.; Salcedo, R.; Manero, O.; Cedillo, G.; Velasco, V. M.; Guzman, M. T.; Fritsch, D.; Khalizov, A. F. *Macromol. Rapid Commun.* **2007,** 28, (2), 183-187.

145. Cruz, A. R.; Zolotukhin, M. G.; Morales, S. L.; Cardenas, J.; Cedillo, G.; Fomine, S.; Salmon, M.; Carreon-Castro, M. P. *Chem. Commun.* **2009,** -, (29), 4408-4410.

146. Hernández-Cruz, O.; Zolotukhin, M. G.; Fomine, S.; Alexandrova, L.; Aguilar-Lugo, C.; Ruiz-Treviño, F. A.; Ramos-Ortíz, G.; Maldonado, J. L.; Cadenas-Pliego, G. *Macromolecules* **2015,** 48, (4), 1026-1037.

147. Segawa, Y.; Higashihara, T.; Ueda, M. *J. Am. Chem. Soc.* **2010,** 132, (32), 11000-11001.

148. Maurya, S.; Noh, S.; Matanovic, I.; Park, E. J.; Narvaez Villarrubia, C.; Martinez, U.; Han, J.; Bae, C.; Kim, Y. S. *Energy Environ. Sci.* **2018,** 11, (11), 3283-3291.

149. Park, E. J.; Kim, Y. S. *J. Mater. Chem. A* **2018,** 6, (32), 15456-15477.

150. Guzmán-Gutiérrez, M. T.; Nieto, D. R.; Fomine, S.; Morales, S. L.; Zolotukhin, M. G.; Hernandez, M. C. G.; Kricheldorf, H.; Wilks, E. S. *Macromolecules* **2011,** 44, (2), 194-202.

151. Klumpp, D. A.; Garza, M.; Jones, A.; Mendoza, S. *J. Org. Chem.* **1999,** 64, (18), 6702-6705.

152. Conroy, J. L.; Sanders, T. C.; Seto, C. T. *J. Am. Chem. Soc.* **1997,** 119, (18), 4285-4291.

153. Jeon, J. Y.; Umstead, Z.; Kangovi, G. N.; Lee, S.; Bae, C. *Top. Catal.* **2018,** 61, (7-8), 610-615.

154. De Vynck, V.; Goethals, E. J. *Macromol. Rapid Commun.* **1997,** 18, (2), 149-156.

155. Cowie, J. M. K. G.; Arrighi, V., *Polymers: chemistry and physics of modern materials*. CRC Press: Taylor & Francis, 2008; pp 240-243.

156. Nuñez, S. A.; Hickner, M. A. *ACS Macro Lett.* **2013,** 2, (1), 49-52.

157. Kreuer, K.-D.; Jannasch, P. *J. Power Sources* **2018,** 375, 361-366.

158. Park, E. J.; Maurya, S.; Hibbs, M. R.; Fujimoto, C. H.; Kreuer, K.-D.; Kim, Y. S. *Macromolecules* **2019,** 52, (14), 5419-5428.

159. Lai, A. N.; Hu, P. C.; Zheng, J. W.; Zhou, S. F.; Zhang, L. *Int. J. Hydrog. Energy* **2019,** 44, (44), 24256-24266.

160. Longworth, R.; Vaughan, D. J. *Nature* **1968,** 218, (5136), 85-87.

161. Gebel, G.; Diat, O. *Fuel Cells* **2005,** 5, (2), 261-276.

162. Dautzenberg, H.; Görnitz, E.; Jaeger, W. *Macromol. Chem. Phys.* **1998,** 199, (8), 1561-1571.

163. Cospito, G.; Illuminati, G.; Lillocci, C.; Petride, H. *J. Org. Chem.* **1981,** 46, (14), 2944-2947.

164. Cerichelli, G.; Illuminati, G.; Lillocci, C. *J. Org. Chem.* **1980,** 45, (20), 3952-3957.

165. Illuminati, G.; Lillocci, C. *J. Org. Chem.* **1977,** 42, (13), 2201-2203.

166. Booth, H.; Bostock, A. H.; Franklin, N. C.; Griffiths, D. V.; Little, J. H. *J. Chem. Soc. Perkin Trans. II* **1978**, (9), 899-907.

167. Cotanda, P.; Petzetakis, N.; Jiang, X.; Stone, G.; Balsara, N. P. *J. Polym. Sci., Part A: Polym. Chem.* **2017,** 55, (13), 2243-2248.

168. Strasser, D. J.; Graziano, B. J.; Knauss, D. M. *J. Mater. Chem. A* **2017,** 5, (20), 9627-9640.

169. Knauss, D. M., Strasser, D. J. Functionalized Poly(diallylpiperidinium) and its Copolymers for Use in Ion Conducting Applications. U.S. Patent Application 20190060842, 2019.

170. Pham, T. H.; Olsson, J. S.; Jannasch, P. *J. Mater. Chem. A* **2019,** 7, (26), 15895-15906.

171. Kang, N. R.; Pham, T. H.; Jannasch, P. *ACS Macro Lett.* **2019,** 8, (10), 1247-1251.

172. Wang, L.; Brink, J. J.; Varcoe, J. R. *Chem. Commun.* **2017,** 53, (86), 11771-11773.

173. Carlson, A.; Eriksson, B.; Olsson, J. S.; Lindbergh, G.; Lagergren, C.; Jannasch, P.; Wreland Lindström, R. *Sustain. Energ. Fuels* **2020**.

Printed by Media-Tryck, Lund 2020 NORDIC SWAN ECOLABEL 3041 0903

LUND UNIVERSITY

ISBN 978-91-7422-738-3

Centre for Analysis and Synthesis
Department of Chemistry
Faculty of Engineering
Lund University

9 789174 227383